

## Development of a foraminifera-based transfer function in the Basque marshes, N. Spain: Implications for sea-level studies in the Bay of Biscay

Eduardo Leorri <sup>a,c,\*</sup>, Benjamin P. Horton <sup>b</sup>, Alejandro Cearreta <sup>c</sup>

<sup>a</sup> Laboratoire d'Etude des Bio-indicateurs Actuels et Fossiles, Université d'Angers-UFR Sciences, 2 Boulevard Lavoisier, 49045, Angers Cedex, France

<sup>b</sup> Sea Level Research Laboratory, Department of Earth and Environmental Science, University of Pennsylvania, 240 South 33rd Street, Philadelphia, PA, 19104, USA

<sup>c</sup> Departamento de Estratigrafía y Paleontología, Facultad de Ciencia y Tecnología, Universidad del País Vasco/EHU, Apartado 644, 48080 Bilbao, Spain

### ARTICLE INFO

#### Article history:

Received 2 May 2007

Received in revised form 23 December 2007

Accepted 3 February 2008

#### Keywords:

marsh foraminifera

transfer function

<sup>137</sup>Cs, Pb concentrations, and <sup>210</sup>Pb dating

sea level

Bay of Biscay

### ABSTRACT

In order to reconstruct former sea level we have developed a foraminifera-based transfer function using three models based on a modern dataset of 59 samples and 23 species obtained from four Basque marshes in Northern Spain. The relationship between observed and foraminifera-predicted elevation illustrated the strong performance of the transfer function ( $r^2_{\text{jack}}$  ranges from 0.74 to 0.81). These results indicated that precise reconstructions of former sea levels are possible (error ranges from 0.11 to 0.19 m). The transfer function was used to calibrate the foraminiferal assemblages collected from a 50 cm salt marsh core. We placed the foraminifera-based reconstructions into a temporal framework using <sup>137</sup>Cs, Pb concentrations, and <sup>210</sup>Pb-derived sediment accumulation rates. The resulting relative sea-level curve is in good agreement with regional tide-gauge data. Both instrumental data and microfossil records suggest a rate of relative sea-level rise of approximately 2 mm yr<sup>-1</sup> for the 20th century.

© 2008 Elsevier B.V. All rights reserved.

### 1. Introduction

High quality relative sea-level data (RSL) reveal spatial and temporal variations in crustal movements, which are used for many applications, ranging from calibrating models of earth rheology and ice sheet reconstructions to the development of coastal lowlands and human occupation. Current concerns regarding the potential eustatic sea-level rise associated with anthropogenic warming of the atmosphere and oceans and its impacts on coastal resources have resulted in increased interest in former RSL fluctuations (IPCC, 2007). RSL predictions will be used as a key variable in future modeling experiments designed to assess coastal response to sea-level variations at a range of spatial scales to inform national and regional hazard assessment and local geomorphological responses where RSL interacts with sediment supply and wind/wave processes (e.g., Kelly et al., 2005). Rates of sea-level rise obtained represent the fundamental basis for comparison with the historical and present day changes. They provide a benchmark against which one must measure the additional sea-level rise that has occurred over the last 100–150 yr (Church and White, 2006; Holgate, 2007).

The global sea-level rise (GSLR) of the last 100–150 yr is affected by two main factors: thermal expansion, with higher water temperatures leading to an increase in ocean volume at constant mass; and the mass of the ocean, as water is exchanged with glaciers and land-grounded ice

caps (Cazenave and Nerem, 2004). Based on historical tide gauge data (>50 yr) GSLR rates approximate 1.8 mm yr<sup>-1</sup> (range 1.7–2 mm yr<sup>-1</sup>; Douglas, 1995, 1997; Peltier and Jiang, 1997; Douglas, 2001; Church et al., 2004; Church and White, 2006). Since 1993 satellite altimetry data have been available and provide estimates of ~3 mm yr<sup>-1</sup> (Cabanes et al., 2001; Cazenave and Nerem, 2004; Leuliette et al., 2004).

To our knowledge, only Tel and García (2001) and Marcos et al. (2005) addressed the recent (1943–2001) sea-level change in the northern Spain, using data from the tide gauges with longer records in the area (Vigo, in the Atlantic coast and La Coruña and Santander, in the southern Bay of Biscay; Table 1). Tel and García (2001) inferred a rate of 2.08 mm yr<sup>-1</sup> for the relative SLR (2.32 mm yr<sup>-1</sup> after removing post-glacial rebound) in agreement with the sea-level trends provided by Marcos et al. (2005). Additionally, Marcos et al. (2007) have analyzed sea-level time series derived from TOPEX altimeter and from tide gauges in the Bay of Biscay over the period 1993–2002. Mean sea-level rise provided by TOPEX altimeter data was 3.09±0.21 mm yr<sup>-1</sup>, which is similar to the rate of GSLR, while tide gauges provided a mean value of 3.89±0.62 mm yr<sup>-1</sup> (2.01±0.85 mm yr<sup>-1</sup> after correcting for vertical land movements using GPS records).

Recently the GSLR dataset currently being produced on the time dependence of the gravitational field of the planet by the Gravity Recovery and Climate Experiment (GRACE) dual satellite measurement system (e.g., Velicogna and Wahr, 2005, 2006; Wahr et al., 2006) has detected an ice mass loss of 248±36 km<sup>3</sup> yr<sup>-1</sup>, equivalent to a GSLR of 0.5±0.1 mm yr<sup>-1</sup> between April 2002 to April 2006, which represents a 250% increase in the rate of ice loss between the periods April 2002 to April 2004 and May 2004 to April 2006 (Velicogna and

\* Corresponding author. Departamento de Estratigrafía y Paleontología, Facultad de Ciencia y Tecnología, Universidad del País Vasco/EHU, Apartado 644, 48080 Bilbao, Spain.  
E-mail address: [eduleorri@yahoo.es](mailto:eduleorri@yahoo.es) (E. Leorri).

**Table 1**  
Tide-gauge data from the Bay of Biscay

Station name	Range of years		Trend and standard error in mm/yr	Corrected trend mm/yr	Geographical location	
	Start	End			Latitude	Longitude
<i>Data from the Permanent Service for Mean Sea Level web site (www.pol.ac.uk)</i>						
Brest	1807	2000	0.99±0.05		48°23' N	4°30' W
Socoa/ St Jean de Luz	1966	1996	1.52±0.69		43°24' N	1°41' W
Pasajes	1948	1962	5.28±2.39		43°19' N	1°55' W
Santander	1944	2001	2.18±0.41		43°28' N	3°48' W
La Coruña	1944	2000	1.25±0.33		43°22' N	8°24' W
<i>Data from Tel and García (2001)</i>						
Santander	1944	1999	1.75	2.05 <sup>a</sup>	43°28' N	3°48' W
La Coruña	1944	1999	1.34	1.49 <sup>a</sup>	43°22' N	8°24' W
Regional (N. Spain)	1943	1999	2.08	2.32 <sup>a</sup>		
<i>Data from Marcos et al. (2005)</i>						
Santander	1943	2001	2.06±0.09	2.12±0.09 <sup>b</sup>	43°28' N	3°48' W
La Coruña	1943	2001	1.46±0.09	2.51±0.09 <sup>b</sup>	43°22' N	8°24' W

<sup>a</sup> Removing post-glacial rebound.

<sup>b</sup> Correction of inconsistency of data and removing post-glacial rebound.

Wahr, 2006). These differences could be related to the acceleration in sea-level rise ( $0.013 \pm 0.6 \text{ mm yr}^{-2}$ ) found by Church and White (2006) for the period 1870–2000, or represent decadal variability (Nerem et al., 2006). In addition, the heterogeneous and limited coverage of historical tide gauges does not capture the regional variability, and hence could not provide a meaningful estimate of the average GSLR

for the past century (Cabanes et al., 2001). Finally, depending on the period considered and the length of the tide-gauge record, the “sign” of the sea-level trend may change (Douglas, 2001).

An important question to address is to identify when the actual rate of sea-level rise began. Based on the data provided by Woodworth (1990), Douglas (2001) stated that sea level began to rise at the modern rate approximately at the middle of the 19th century. Nevertheless, Barnett (1984) and Peltier and Tushingham (1989) estimated a much higher rate ( $\sim 2.3 \text{ mm yr}^{-1}$ ) after the 1920s than those reported for longer periods including data from the 19th century (i.e.  $\sim 1.4 \text{ mm yr}^{-1}$ ; Barnett, 1984). Recent geological-based research from the western margins of the North Atlantic has provided the first indication that modern rates of RSL rise (last 100 yr) in this region may be more rapid than the long-term rate of rise (over the last 800–1000 yr), and that the timing of this acceleration may be indicative of a link with human-induced climate change (Gehrels et al., 2002; Donnelly et al., 2004; Gehrels et al., 2004, 2005). No such data exists for areas on the eastern margins of the North Atlantic and this paper seeks to address this imbalance by providing high-quality data from the Bay of Biscay (Fig. 1) to examine the issue of recent changes in the rate of RSL rise.

### 1.1. Foraminifera-based transfer functions

Advances in high-resolution sea-level reconstruction have been made in the last few years through the development of foraminifera-based transfer functions (Gehrels et al., 2002; Edwards et al., 2004; Gehrels, 2004; Hayward et al., 2004; Horton and Edwards, 2006; Boomer and Horton, 2006). Fossil foraminifera have been used as “proxies” for elevation by quantifying the relationship between faunal data (relative abundance of individual species) and environmental

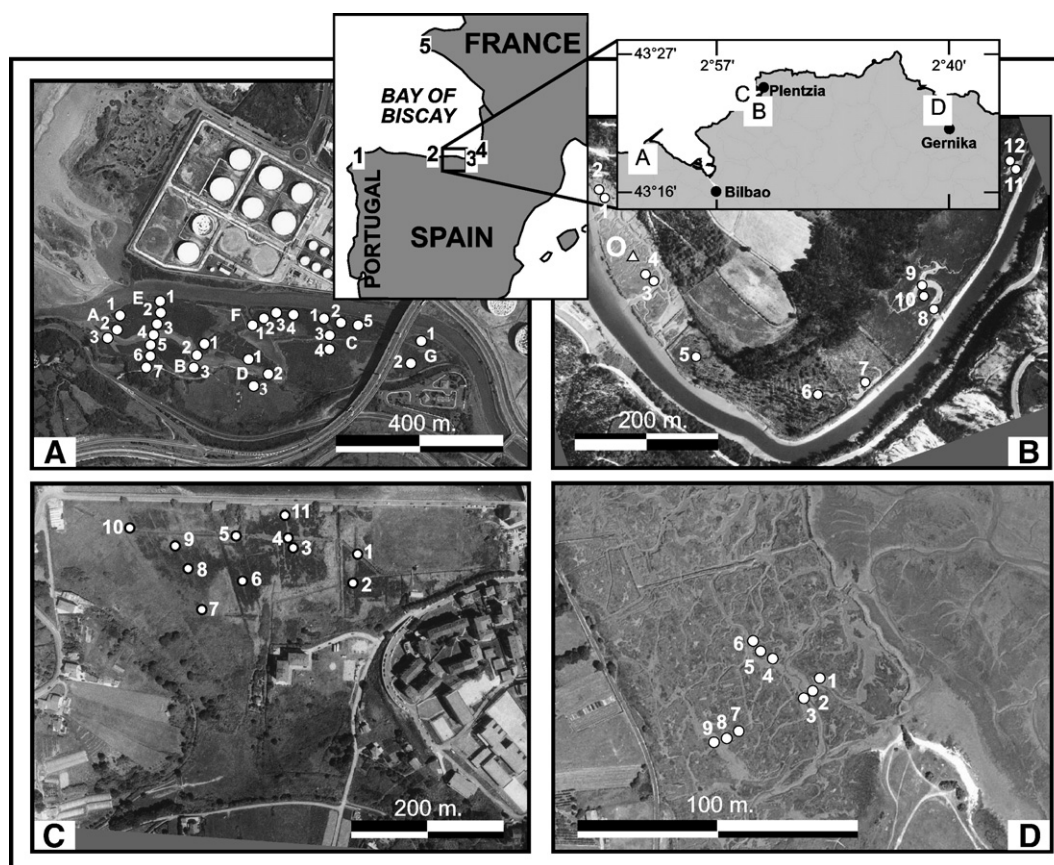


**Fig. 1.** Location of the four Basque marshes, sample sites and localities referred to in the text. Key: A—Muskiz marsh (Barbadun estuary); B—Ostrada marsh (Plentzia estuary); C—Txipio marsh (Plentzia estuary); D—Axpe-Busturia marsh (Urdaibai estuary); 1—La Coruña; 2—Santander; 3—Pasajes; 4—Socoa/St Jean de Luz; 5—Brest. White dots indicate surficial samples analyzed for foraminifera. White triangle indicates short core analyzed for foraminifera.

data (elevation) in the modern environment. Although many local habitat factors (e.g., Hippensteel et al., 2000, 2002) influence the composition of foraminiferal assemblages, studies from North America (Scott and Leckie, 1990), South America (Jennings et al., 1995) and Europe (Gehrels et al., 2001; Gehrels and Newman, 2004; Horton and Edwards, 2006) indicate that the strong correlation between foraminiferal assemblage zones distribution and marsh elevation can be recognized worldwide. These modern relationships are then applied to cores to reconstruct past tide levels from fossil assemblages within sedimentary sequences in order to reconstruct paleomarsch-surface elevation.

Cearreta et al. (2002) established that marsh foraminifera from the Basque marshes (southern Bay of Biscay) were sensitive to both elevation above mean sea level and salinity. In this paper, we present a transfer function developed from the modern distributions of foraminifera recorded in four Basque marshes: Muskiz marsh (Barbadun estuary), Ostrada and Txipio marshes (Plentzia estuary), and Axpe–Busturia marsh (Urdaibai estuary) in the North of Spain (Fig. 1). We describe the development and application of this transfer function, and assess its performance in reconstructing paleomarsch-surface elevation from one short core (50 cm) taken in the Ostrada marsh (Fig. 1). We compare the reconstructed paleomarsch-surface elevation with regional tide-gauge data in order to provide the first quantitative assessment of the potential of intertidal foraminifera for RSL studies in the Bay of Biscay.

## 2. Regional setting

Marshes in the northern coast of Spain are few and fragmentary. They are restricted to the inner parts of the small estuaries that sporadically interrupt the continuous cliffs that characterize this coastal area (Cearreta et al., 2002). Furthermore, marsh reclamation for agricultural and disease-eradication purposes was initiated in the 17th century, and was particularly intense since the second half of the 19th century. However, during the last few decades agriculture has been in decline and thus cultivated areas have been abandoned. The lack of dyke maintenance has allowed tidal estuarine water to invade these once artificially isolated areas and, consequently, halophytic vegetation is rapidly recolonizing them (Cearreta et al., 2002). All four study sites (Muskiz, Ostrada, Txipio and Axpe–Busturia marshes) come from estuaries (Barbadun, Plentzia and Urdaibai) with similar mesotidal ranges (2.5 m) (Gobierno Vasco, 1986; Villate et al., 1990; Madariaga, 1995; Valencia et al., 2004; Valencia and Franco, 2004).

The Barbadun estuary forms the tidal part of the Barbadun river. This estuary has a total surface of 204 ha, a length of 4.4 km and an average width between 5 and 10 m (Gobierno Vasco, 1999). The Muskiz marsh (Fig. 1A) is located in the middle reaches of the Barbadun estuary and consists of halophytic plants: *Sarcocornia perennis*, *Sarcocornia fruticosa* and *Salicornia ramossissima* together with *Atriplex portulacoides* and *Puccinellia maritima* among others (Gobierno Vasco, 1996).

The Plentzia estuary forms the tidal part of the Butron river. The estuary has a total surface of 115 ha, a length of 7 km and an average width of 20 m (Gobierno Vasco, 1998). The Ostrada marsh (Fig. 1B) is located in the upper Plentzia estuary, limited inland by wooded uplands and can be subdivided into: high marsh covered by *Arthrocnemum fruticosum*, *Juncus maritimus* and *Limonium binervosum*; middle marsh, which is colonized by *Spergularia maritima* and *S. ramossissima*; and a low marsh consisting of *Spartina maritima*, *S. ramossissima*, *L. binervosum* and *A. portulacoides* (Cearreta et al., 2002). There are no additional fresh water discharges onto the marsh from the surrounding uplands except for surficial run-off. The Txipio marsh is located in the lower Plentzia estuary (Fig. 1C). A fresh water stream enters the marsh from the south and its course marks the limit between the marsh and the uplands on the west side. Thirteen halophytic plant species were found in Txipio by Onaindia

and Amezaga (1999). *A. fruticosum*, *Aster tripolium*, *A. portulacoides*, *J. maritimus*, *Polygonum maritimum*, *P. maritima*, *S. ramossissima* and *Spartina maritima* are dominant in the low marsh, whereas *Elymus pycnanthus* and *Phragmites australis* dominate the high marsh.

The Urdaibai estuary is formed by the tidal part of the Oka river. The estuary covers an area of 22,000 ha, and occupies the flat bottom of the 12.5 km long, 1 km wide alluvial valley. The Axpe–Busturia marsh (Fig. 1D) is located in the middle reaches of the estuary and is characterized by *A. portulacoides* and *P. maritima* vegetation (Benito and Onaindia, 1991; Uriarte et al., 2005).

## 3. Materials and methods

We collected seasonal surface sediment samples for micropaleontological analysis from 27 sites in the Muskiz marsh (year 2000), 12 sites in the Ostrada marsh (year 1997), 11 sites in the Txipio marsh (year 1997) and 9 sites in the Axpe–Busturia marsh (year 2003). We chose sampling sites that were representative of different marsh

**Table 2**  
Ostrada core bulk density (g cm<sup>-3</sup>)

Sample	Bulk density (g cm <sup>3</sup> )
O#1	0.7993
O#2	0.7801
O#3	0.7121
O#4	0.8390
O#5	0.8809
O#6	0.8615
O#7	0.8747
O#8	0.9467
O#9	0.8015
O#10	0.7667
O#11	0.8281
O#12	0.6860
O#13	0.7995
O#14	0.8729
O#15	0.9462
O#16	0.7803
O#17	0.9235
O#18	0.8512
O#19	0.9018
O#20	0.7993
O#21	0.7958
O#22	0.9119
O#23	0.8790
O#24	0.8152
O#25	0.8972
O#26	0.8230
O#27	0.9341
O#28	0.7370
O#29	1.1269
O#30	1.0767
O#31	1.0434
O#32	0.9589
O#33	0.8772
O#34	1.1599
O#35	0.9625
O#36	0.8682
O#37	0.9036
O#38	0.9923
O#39	0.9715
O#40	0.8320
O#41	0.8698
O#42	1.1274
O#43	0.9511
O#44	1.0715
O#45	1.0930
O#46	0.8669
O#47	0.8507
O#48	1.0698
O#49	0.8515
O#50	1.0277

subenvironments in terms of elevation above mean sea level and distance from the main estuarine channel, including different vegetated and unvegetated areas (Fig. 1).

A 50 cm sediment core was collected from the Ostrada marsh (year 1997). Aerial and historical photography indicate that the selected area does not have a history of reclamation. Furthermore, sedimentological investigations did not reveal any agricultural layers that have been identified in many other salt marshes in Northern Spain (e.g., Cearreta et al., 2002). The core was extruded from a small-unvegetated area surrounded by halophytic vegetation (*Atriplex fruticosum*, *J. maritimum* and *L. binervosum*) within the central part of the marsh (Fig. 1B). Two PVC tubes (12.5 cm diameter) were inserted into the sediment in order to obtain sufficient material to determine the benthic foraminifera, sediment geochemistry (including Pb concentrations), and  $^{137}\text{Cs}$  and  $^{210}\text{Pb}$  geochronologies. The core was described, photographed and X-radiographed before being sliced into 1 cm increments.

We measured topographic elevation (Leica station; elevation error:  $\pm 0.005$  m) for all modern samples and the core and this information is presented relative to the local ordnance datum (lowest tide at the Bilbao Harbour on 27th September 1878). Although each estuary has a similar tidal range, the physiographic conditions differ, thus the inundation frequency at each study area must be calculated. We therefore measured tides at each field site and compared them with the closest tide gauge and standardized elevations relative to the tidal range. Hence, the elevations are expressed as a standardized water level index (SWLI; Horton et al., 1999; Hamilton and Shennan, 2005):

$$\text{SWLI}_n = \frac{100(h_n - h_{\text{MSL}})}{h_{\text{MHHW}} - h_{\text{MSL}}} + 100$$

where  $\text{SWLI}_n$  is the standardized water level index for sample  $n$ ,  $h_n$  the elevation of sample  $n$  (m above local ordnance datum),  $h_{\text{MSL}}$  the mean sea-level elevation (m above local ordnance datum),  $h_{\text{MHHW}}$  the mean higher high water elevation (m above local ordnance datum). This produces a standardized water level index (SWLI) for each modern sample with 100 representing mean sea level and 200 for mean higher high water. SWLI for each fossil sample is then converted back to an elevation above local ordnance datum at the field site by reversing the calculations (Horton et al., 1999; Hamilton and Shennan, 2005).

Although compaction of the sediment during sampling was negligible (Cearreta et al., 2002), we must consider that auto-compaction (loss of porosity due to the load of overlying sediments) can introduce a significant error into sea-level estimations (Paul and Barras, 1998; Pizzuto and Schwedendt, 1997). Organic material and fine-grained sediments can undergo significant volume reduction, whereas siliceous gravels and sands are almost incompressible (Allen, 1999). Cores obtained in the Plentzia estuary indicate that the depth of the contact between Holocene sediments and the basement (Mesozoic–Cenozoic rocks) varies from 8 to 20 m from the upper to lower estuary. These sediments are composed mainly by gravels and sand (Leorri and Cearreta, 2004). The salt marsh sediments are between 0.5 m and 1 m thick and composed of clay ( $70.4 \pm 5.4\%$ ; average  $\pm$  SD) and silt ( $21 \pm 2.6\%$ ) with small amount of sand ( $8.5 \pm 6.7\%$ ), and very low content in organic matter ( $1.9 \pm 0.3\%$ ). Thus, the thin marsh lithosome, the dominance of minerogenic sediments, and the proximity to the basal contact with Mesozoic–Cenozoic rocks provide little opportunity for additional accommodation space due to auto-compaction and therefore, we have considered it to be minimal. This is also supported by bulk density data (Table 2). The core shows some variability towards its base, however, related to an increase in sand content rather than compaction.

### 3.1. Modern and fossil microfaunal study

We extruded two subsamples of  $40 \text{ cm}^2$  at each sampling site by pressing down a hard plastic ring into the surface layer. The top

1–2 cm of oxygenated sediment was placed in a bottle containing ethanol for analysis. Infaunal population of agglutinated foraminifera has been reported from North American marshes of the Atlantic coast at depths up to 60 cm (e.g., Goldstein et al., 1995; Hippensteel et al., 2000). Although similar infaunal distribution has been reported from the French Atlantic coast (Duchemin et al., 2005), our analysis from Plentzia estuary (unpublished data) suggest that infaunal living individuals are concentrated in the uppermost interval (0–2 cm) and do not significantly change the assemblage downcore. This conclusion is also supported by numerous other studies (e.g., Patterson et al., 2004; Culver and Horton, 2005; Tobin et al., 2005).

We sieved modern samples through a 1 mm (to remove large organic fragments) and a 63-micron sieve and washed to remove clay and silt material. Samples were stained using rose Bengal (Walton, 1952; Murray and Bowser, 2000) in order to identify specimens considered to be alive at the time of collection. We picked tests until a representative number of more than 300 individuals for each assemblage (live and dead) was obtained and then studied under a stereoscopic binocular microscope using reflected light. A sum of 52,300 foraminifera was identified from surface sediments (Appendix A). All foraminiferal species identified in the samples are listed in Appendix A and species relative abundances ( $>2\%$ ) are presented in Table 3. The live (stained) assemblages are supposedly in equilibrium with the environment, thus they vary through the year depending on the variation of the environmental parameters (Murray, 1991). On the other hand, the dead assemblages (unstained) represent a time-averaged accumulation of foraminiferal tests (Murray, 1991). Thus, we consider the dead assemblages to be a better analogue for reconstructing the former sea level (Horton, 1999; Horton and Edwards, 2003; Horton et al., 2005; Horton and Edwards, 2006). Horton and Edwards (2003) and Horton and Murray (2006) suggested that the transfer function improves when multiple samples are accumulated because of the high variability (“patchiness”) of the foraminiferal distribution (Buzas et al., 2002). In order to avoid this variability, dead assemblages of the two replicates ( $40 \text{ cm}^2$  each) and seasonal samples were averaged for each sampling site.

We analyzed the samples of the Ostrada core for foraminiferal content at 1 cm intervals following the same procedure described above for modern samples, except that they were not stained. The number of samples analyzed in this core was 35, and more than 10,800 foraminifera were identified. All foraminiferal species identified in the core samples are listed in Appendix A and species relative abundances ( $>2\%$ ) are presented in Table 4.

### 3.2. Ostrada core age model

Recent sedimentation trends (ca. 1850 AD to present) typically employ shorter-lived radionuclides ( $^{210}\text{Pb}$ ,  $^{137}\text{Cs}$ ).  $^{210}\text{Pb}$  is a naturally occurring radionuclide which vertical distribution allows ages to be ascribed to sedimentary layers based on the known decay rate of  $^{210}\text{Pb}$  (see Appleby and Oldfield (1992) for a discussion of the  $^{210}\text{Pb}$  method), this technique is restricted to the last 120 yr (Gottgens et al., 1999) and needs to be supported by other chronological markers (Smith, 2001).  $^{137}\text{Cs}$  (half life 30 yr) is an artificially produced radionuclide present in the environment since 1954. Its presence in the study area is likely to be dominantly derived from nuclear weapons testing, with peak fallout in 1963, which can be used to derive rates of sediment accretion (e.g., Ritchie and McHenry, 1990; Cundy and Croudace, 1996; Cundy et al., 1998). However, the use of  $^{137}\text{Cs}$  fallout peaks is increasingly viewed as uncertain due to post depositional migration (Abril, 2004). Therefore, we also analyzed Pb concentrations to further support this chronology. Heavy metal pollution and Pb concentrations are recently being used as chronological markers in high-resolution sea-level studies (e.g., Donnelly et al., 2004; Gehrels et al., 2006). In

**Table 3**  
Relative abundance (>2%) of foraminiferal species in the dead assemblages of surficial samples from the Basque marshes

Sample	<i>Ammonia tepida</i>	<i>Arenoparrella mexicana</i>	<i>Aubignyna hamblensis</i>	<i>Brizalina britannica</i>	<i>Cibicides lobatulus</i>	<i>Cibicides pseudoungerianus</i>	<i>Criboelphidium oceanensis</i>	<i>Criboelphidium williamsoni</i>	<i>Fissurina lucida</i>	<i>Haynesina germanica</i>	<i>Jadammina macrescens</i>	<i>Massilina secans</i>
O-1	20.2	0.9	9.4	0.9	0.3	0.0	3.4	3.6	1.9	39.3	15.6	0.0
O-2	19.3	0.5	6.9	0.2	0.0	0.0	0.9	4.3	2.8	44.9	14.2	0.0
O-3	19.9	0.9	6.0	0.2	0.0	0.0	2.9	3.4	0.9	22.2	29.3	0.0
O-4	0.3	1.5	0.0	0.0	0.0	0.0	0.0	0.3	0.0	0.5	82.6	0.0
O-5	0.5	1.9	0.0	0.0	0.0	0.0	0.2	1.3	0.0	1.0	39.6	0.0
O-6	13.6	0.3	0.5	0.0	0.0	0.0	0.4	3.9	0.0	3.8	64.0	0.0
O-7	18.5	1.2	6.9	1.8	0.0	0.0	6.2	2.0	1.4	29.6	17.0	0.0
O-8	19.8	0.5	6.6	3.0	0.2	0.0	12.2	1.6	1.9	26.7	14.3	0.0
O-9	17.0	0.9	2.6	0.7	0.0	0.0	6.9	2.2	2.3	36.3	15.6	0.0
O-10	0.0	1.2	0.0	0.0	0.0	0.0	0.0	0.0	0.0	0.2	66.3	0.0
O-11	15.4	0.2	5.6	0.2	0.0	0.0	8.0	2.0	0.2	46.7	11.4	0.0
O-12	5.4	0.8	0.2	0.0	0.0	0.0	1.8	0.8	0.0	5.4	40.6	0.0
TX1	22.9	1.3	8.5	0.8	0.6	0.0	3.0	9.9	0.4	25.6	10.1	0.0
TX10	17.6	3.5	6.1	0.0	0.2	0.0	5.1	8.3	1.0	14.2	18.3	0.0
TX11	41.0	2.7	0.2	0.4	1.6	0.0	3.9	10.3	0.0	8.7	9.5	0.2
TX2	23.8	1.0	2.2	0.0	0.0	0.0	7.2	11.5	0.2	11.9	8.0	0.0
TX3	36.0	1.5	2.1	0.0	0.0	0.0	4.7	6.4	0.0	11.2	11.5	0.0
TX4	31.9	0.6	9.1	0.0	0.0	0.0	2.3	9.2	0.3	28.8	6.2	0.0
TX5	18.0	1.3	9.7	0.2	0.0	0.0	3.9	6.5	1.2	13.3	23.7	0.0
TX6	24.4	1.0	1.7	0.0	0.0	0.0	1.4	8.4	0.0	1.2	45.5	0.0
TX7	6.8	1.4	0.6	0.0	0.0	0.0	0.0	1.7	0.0	0.0	37.6	0.0
TX8	0.0	3.3	0.0	0.0	0.0	0.0	0.0	0.0	0.0	0.0	48.1	0.0
TX9	39.0	0.5	5.0	0.0	0.0	0.0	3.7	15.6	0.0	12.0	10.7	0.0
AB1	0.0	0.0	0.0	0.0	0.0	0.0	0.0	1.5	0.0	0.3	87.9	0.0
AB2	13.2	0.0	0.0	0.0	0.7	0.0	0.0	10.3	0.0	51.3	12.9	0.0
AB3	15.0	0.0	0.0	0.0	10.0	0.0	1.0	16.6	0.0	42.9	2.3	1.0
AB4	1.6	0.0	0.0	0.0	0.0	0.0	0.0	0.0	0.0	0.3	72.8	0.0
AB5	8.3	0.0	0.0	0.0	3.7	0.0	2.0	6.7	0.0	28.0	27.3	0.0
AB6	15.2	0.0	0.0	0.0	5.0	0.0	0.3	9.9	0.0	47.0	9.9	0.0
AB7	0.0	0.0	0.0	0.0	0.0	0.0	0.0	0.0	0.0	0.0	81.2	0.0
AB8	5.2	0.0	0.0	0.0	0.3	0.0	0.0	4.5	0.0	12.3	57.3	0.0
AB9	6.2	0.0	0.0	0.0	0.7	0.0	0.0	4.2	0.0	29.3	51.8	0.0
A1	2.8	0.0	0.0	0.3	49.2	0.0	0.0	4.4	0.0	1.6	2.5	1.3
A2	24.3	0.0	0.0	1.4	12.2	1.4	0.0	3.6	0.0	0.6	41.7	0.3
A3	11.9	0.0	0.0	0.3	1.7	3.1	0.0	2.5	0.0	0.9	56.4	0.0
B1	1.5	0.0	0.0	0.3	44.3	0.0	0.3	0.0	0.0	2.4	2.8	6.1
B2	4.1	0.0	0.0	1.9	18.5	0.0	0.0	0.3	0.0	5.4	29.8	1.2
B3	0.0	0.0	0.0	0.0	0.3	0.0	0.0	0.0	0.0	0.0	55.3	0.0
C1	10.1	0.0	0.0	2.1	0.6	0.0	0.0	0.6	0.3	8.9	61.5	0.0
C2	0.6	0.0	0.0	0.0	0.0	0.0	0.0	0.0	0.0	0.0	50.4	0.0
C3	26.3	0.0	0.0	0.0	0.3	0.0	0.0	0.6	0.0	0.9	57.1	0.0
C4	5.7	0.0	0.0	0.0	0.0	0.0	0.0	0.3	0.0	0.0	44.8	0.0
D1	14.4	0.0	0.0	0.3	17.6	0.0	5.0	2.2	0.0	13.2	7.2	0.0
D2	13.9	0.0	0.0	2.5	10.1	0.0	1.6	1.6	0.0	4.1	40.2	0.3
D3	32.0	0.0	0.0	0.0	2.9	0.0	0.0	1.5	0.0	2.1	53.4	0.3
E1	4.5	0.0	0.0	4.5	14.6	0.0	0.0	0.3	0.0	3.6	4.2	0.0
E2	9.5	0.0	0.0	1.9	26.0	0.0	0.3	0.6	0.0	2.8	6.7	2.2
E3	10.1	0.0	0.0	3.2	31.0	0.0	0.0	1.6	0.0	6.6	9.2	0.3
E4	1.2	0.0	0.0	0.0	0.6	0.0	0.0	0.0	0.0	0.6	67.7	0.0
E5	0.7	0.0	0.0	0.0	0.0	0.0	0.0	0.0	0.0	0.0	57.4	0.2
E6	17.6	0.0	0.0	0.6	8.7	0.0	0.0	0.9	0.0	0.9	43.6	0.9
E7	2.0	0.0	0.0	0.3	56.4	0.0	0.0	0.0	0.0	1.0	0.7	6.2
F1	23.1	0.0	0.0	2.4	21.0	0.0	0.3	1.2	0.0	15.1	12.1	1.2
F2	0.8	0.0	0.0	0.0	0.0	0.0	0.0	0.0	0.0	0.6	73.1	0.0
F3	0.0	0.0	0.0	0.0	0.0	0.0	0.0	0.3	0.0	0.0	54.5	0.0
F4	0.3	0.0	0.0	0.0	0.0	0.0	0.0	0.0	0.0	0.0	83.2	0.0
F5	0.0	0.0	0.0	0.0	0.0	0.0	0.0	0.0	0.0	0.0	40.5	0.0
G1	32.9	0.0	0.0	0.0	0.6	0.0	0.9	0.9	0.0	54.8	7.9	0.0
G2	3.0	0.0	0.0	0.0	0.3	0.0	0.0	0.0	0.0	0.3	86.2	0.0

core sediments Pb concentration maximum has been dated between 1969 and 1975 by numerous authors (e.g., Weiss et al., 1999; Bindler et al., 2001; Eades et al., 2002; Renberg et al., 2002; Farmer et al., 2006), being most likely related to the peak in pollution reached in the early 1970s when increased emission controls and lead-free petrol were introduced (Renberg et al., 2002). The initial divergence of Pb concentrations from background values could be related to the increase of European Pb emissions as result of the Industrial Revolution (~1800 AD). Gehrels et al. (2006) assigned an age of 1820±20 to this change and has been dated in core sediments between 1800 and 1850 (Bindler et al.,

2001; Eades et al., 2002; Renberg et al., 2002). Therefore we will use here 1820±20 as a compromising age.

Sub-samples of ~20 g, at 1 cm intervals, were counted for 10 h in a Canberra well-type, high-resolution gamma ray spectrometer to determine the activities of <sup>137</sup>Cs and other gamma emitters. <sup>210</sup>Pb was determined using the method described by Flynn (1968) where 3 g samples were digested twice with *aqua regia*, and the solutions converted to chlorides prior to autodeposition onto silver discs. The <sup>210</sup>Pb activity (via the <sup>210</sup>Po granddaughter) was then measured using a Canberra Quad alpha spectrometry System. <sup>209</sup>Po was used as an

<i>Miliammina fusca</i>	<i>Miliolinella subrotunda</i>	<i>Planorbolina mediterraneensis</i>	<i>Quinqueloculina lata</i>	<i>Quinqueloculina oblonga</i>	<i>Quinqueloculina seminula</i>	<i>Hormosina moniliforme</i>	<i>Rosalina anomala</i>	<i>Rosalina irregularis</i>	<i>Textularia earlandi</i>	<i>Trochammina inflata</i>	Elevation (m)
0.2	0.0	0.0	0.0	0.0	2.5	0.3	0.0	0.0	0.0	1.2	2.419
0.2	0.0	0.0	0.0	0.0	3.3	0.6	0.0	0.2	0.0	1.3	3.131
0.5	0.0	0.0	0.0	0.0	3.7	0.9	0.0	0.0	0.2	8.9	3.152
0.2	0.0	0.0	0.0	0.0	0.3	0.0	0.0	0.0	0.0	14.5	3.753
5.0	0.0	0.0	0.0	0.0	0.0	1.6	0.0	0.0	0.0	49.0	3.609
0.0	0.0	0.0	0.0	0.0	0.8	8.4	0.0	0.0	0.0	4.5	3.512
0.3	0.0	0.2	0.0	0.0	4.5	1.5	0.2	0.6	0.0	7.4	2.444
0.8	0.0	0.0	0.0	0.0	7.1	0.3	0.0	1.5	0.0	2.3	2.505
2.7	0.0	0.0	0.0	0.0	1.7	0.7	0.0	0.0	0.0	10.0	3.213
1.7	0.0	0.0	0.0	0.0	4.8	0.0	0.0	0.0	4.3	21.7	4.021
0.4	0.0	0.0	0.0	0.0	0.5	1.6	0.0	0.0	0.0	7.9	2.899
2.4	0.0	0.0	0.0	0.0	1.4	1.2	0.0	0.0	0.0	39.7	3.452
0.3	0.0	0.0	0.0	0.0	4.2	0.5	0.0	0.0	0.0	11.3	2.092
0.3	0.0	0.0	0.0	0.0	5.3	2.2	0.0	0.0	0.0	17.8	2.266
1.0	0.2	0.0	0.0	4.2	1.3	2.4	0.3	0.3	0.3	11.2	2.449
0.0	0.0	0.0	0.0	0.0	2.9	1.7	0.0	0.0	0.0	29.7	2.428
1.1	0.0	0.0	0.0	0.0	6.2	0.7	0.0	0.0	0.2	18.6	2.473
0.5	0.0	0.0	0.0	0.0	2.4	1.5	0.0	0.0	0.0	7.6	2.021
0.9	0.0	0.0	0.0	0.0	5.2	1.9	0.0	0.0	1.4	12.5	2.019
0.3	0.0	0.0	0.0	0.0	0.2	1.7	0.0	0.0	0.0	14.5	2.583
1.4	0.0	0.0	0.0	0.0	0.9	0.0	0.0	0.0	0.0	49.5	2.815
1.3	0.0	0.0	0.0	0.0	0.0	0.0	0.0	0.0	0.0	47.4	2.488
1.5	0.0	0.0	0.0	0.0	3.3	0.8	0.0	0.0	0.2	7.1	2.245
0.0	0.0	0.0	0.0	0.0	1.8	0.0	0.0	0.0	0.0	8.8	3.717
0.0	0.7	0.0	0.0	0.0	4.6	0.0	0.0	0.0	0.0	4.0	3.337
0.0	0.0	0.0	0.0	0.0	3.3	0.0	2.0	0.7	0.0	2.3	2.857
0.6	0.0	0.0	0.0	0.0	0.0	0.0	0.0	0.0	0.0	24.6	3.787
1.3	0.0	0.0	0.0	0.0	1.0	0.0	0.0	0.0	0.0	20.0	3.257
2.0	0.0	0.0	0.0	0.0	1.3	0.0	0.0	0.0	0.0	7.3	2.537
0.0	0.0	0.0	0.0	0.0	0.0	0.0	0.0	0.0	0.0	18.8	3.747
2.6	0.0	0.0	0.0	0.0	2.9	0.0	0.0	0.0	0.0	13.9	3.437
1.3	0.0	0.0	0.0	0.0	1.3	0.0	0.7	0.0	0.0	4.6	3.337
0.0	1.3	0.9	3.1	0.0	7.2	0.0	7.2	8.4	0.0	2.2	3.504
0.3	0.0	0.8	1.4	0.0	1.7	0.0	0.6	1.7	0.0	6.6	4.150
0.0	0.3	0.0	0.0	0.0	4.8	0.0	0.0	0.0	0.0	17.6	4.189
0.0	0.3	1.5	3.7	0.0	3.1	0.0	6.7	19.3	0.0	0.0	3.220
0.0	2.5	1.2	3.4	0.0	2.8	0.0	7.9	12.7	0.0	0.3	4.268
0.0	0.0	0.0	0.0	0.0	0.3	0.0	0.0	0.3	0.0	43.9	4.369
0.0	0.3	0.0	0.0	0.0	0.9	0.0	0.0	3.1	0.0	10.4	3.208
0.0	0.0	0.0	0.0	0.0	0.3	0.0	0.0	0.0	0.0	48.7	4.426
0.0	0.0	0.0	0.0	0.0	0.0	0.0	0.0	0.6	0.0	13.1	4.078
0.0	0.0	0.0	0.0	0.0	0.0	0.0	0.0	0.0	0.0	49.2	4.112
0.0	2.2	1.9	1.9	0.0	14.1	0.0	4.7	6.9	0.0	2.5	3.209
0.0	0.0	0.3	1.0	0.0	4.7	0.0	1.9	8.9	0.0	4.7	3.752
0.0	0.0	0.0	0.0	0.0	0.9	0.0	0.9	0.3	0.0	5.0	4.212
0.0	0.0	1.9	0.3	1.6	5.8	0.0	8.4	40.8	0.0	0.7	3.398
0.3	2.8	4.1	1.3	0.6	6.0	0.0	9.5	20.3	0.0	1.3	3.843
0.0	1.9	0.6	2.5	0.0	5.4	0.0	6.3	13.0	0.0	1.6	3.581
0.9	0.3	0.3	0.0	0.0	0.3	0.0	0.0	1.2	0.0	26.5	4.302
0.9	0.0	0.0	0.0	0.0	14.9	0.0	0.0	0.0	0.0	25.8	4.186
0.6	0.0	0.9	1.2	0.0	1.7	0.0	2.9	4.9	0.0	11.6	4.196
0.0	2.3	0.7	8.5	0.0	5.6	0.0	5.6	3.3	0.0	0.3	3.033
0.3	0.0	0.0	3.3	0.0	3.3	0.0	1.2	6.2	0.0	4.5	3.342
0.0	0.0	0.3	0.0	0.0	0.0	0.0	0.0	0.0	0.0	24.4	4.285
1.3	0.0	0.0	0.0	0.0	0.3	0.0	0.0	0.0	0.0	43.6	4.483
0.3	0.0	0.0	0.0	0.0	0.0	0.0	0.0	0.0	0.0	16.2	4.513
0.0	0.0	0.0	0.0	0.0	0.0	0.0	0.0	0.0	0.0	59.5	4.423
0.3	0.0	0.0	0.0	0.0	0.9	0.0	0.3	0.0	0.0	0.3	3.768
0.0	0.0	0.0	0.0	0.0	0.0	0.0	0.0	0.0	0.0	10.2	4.052

internal standard. Analytical methods for determining Pb concentrations are described in Cearreta et al. (2002).

At the Ostrada core  $^{210}\text{Pb}$  activity shows a general decline with depth, although slight inflections in the activity-depth profile occur at -6 cm and -12 cm (Table 5). These inflections are likely to be caused by a change in sediment accretion rate, as they are not related to changes in core composition, and are also unlikely to be caused by mixing (as the sediment is finely-laminated). Applying the simple model of  $^{210}\text{Pb}$  dating (Robbins, 1978) gives an average accretion rate of 3.7 mm yr<sup>-1</sup> ( $2\sigma$  range=2.7–6.2 mm yr<sup>-1</sup>) over the depth interval 0–35 cm. The

constant rate of supply (CRS) model (Goldberg, 1963) indicates a relatively slow rate of sediment accumulation over the depth interval 15–21 cm (0.6 mm yr<sup>-1</sup>), with more rapid accretion of 3.2 mm yr<sup>-1</sup> over the interval 15–0 cm (Table 5). Constant initial concentration (CIC) model has been rejected since the  $^{210}\text{Pb}$  record is uneven, which prevents its use (Marshall et al., 2007).  $^{137}\text{Cs}$  shows a clear subsurface maximum in activity at -11 cm depth, declining with depth to negligible values at -30 cm. Ascribing this subsurface activity maximum to 1963 gives an accretion rate of 3.2 mm yr<sup>-1</sup>. Pb concentrations increasing from a fairly constant baseline value at depth, attaining a

**Table 4**  
Relative abundances (>2%) of foraminiferal species in the Ostrada core samples

Sample	Depth (m)	Elevation (m)	<i>Ammonia tepida</i>	<i>Arenoparrella mexicana</i>	<i>Aubignyna hamblensis</i>	<i>Criboelphidium oceanensis</i>	<i>Criboelphidium williamsoni</i>	<i>Fissurina lucida</i>	<i>Haynesina germanica</i>	<i>Jadammina macrescens</i>	<i>Miliammina fusca</i>	<i>Trochammina inflata</i>	<i>Hormosina moniliforme</i>
O#1	0.01	3.39	5.2	0.3	0.0	0.0	1.6	0.0	11.0	76.9	0.3	2.3	1.9
O#2	0.02	3.37	0.0	0.3	0.0	0.0	0.0	0.0	0.0	93.5	0.0	5.9	0.3
O#3	0.03	3.36	0.3	9.9	0.0	0.0	0.0	0.0	3.7	62.1	0.9	18.6	4.3
O#4	0.04	3.35	0.0	14.7	0.0	0.0	0.0	0.0	0.3	66.3	0.0	10.9	7.8
O#5	0.05	3.34	0.0	0.0	0.0	0.0	0.0	0.0	0.3	98.1	0.0	1.6	0.0
O#6	0.06	3.33	0.3	13.5	0.0	0.0	0.0	0.0	0.3	58.8	1.3	15.1	10.6
O#7	0.07	3.32	0.0	4.2	0.0	0.0	0.0	0.0	1.3	56.5	0.3	27.5	10.2
O#10	0.10	3.29	0.3	0.0	0.0	0.0	0.0	0.0	1.3	92.2	0.0	6.2	0.0
O#13	0.13	3.26	0.0	5.7	0.0	0.0	0.0	0.0	0.0	50.5	0.0	38.4	5.4
O#14	0.14	3.25	0.0	8.9	0.0	0.0	0.0	0.0	0.3	63.3	0.0	23.4	4.1
O#15	0.15	3.24	0.3	0.8	0.0	0.0	0.6	0.0	5.3	84.0	0.0	7.8	1.1
O#16	0.16	3.23	0.3	11.3	0.0	0.0	0.0	0.0	0.0	66.5	0.6	20.2	1.2
O#17	0.17	3.22	0.0	10.6	0.0	0.0	0.0	0.0	0.6	45.8	1.6	38.5	1.9
O#20	0.20	3.19	0.0	0.6	0.0	0.0	0.0	0.0	0.0	93.1	0.0	5.9	0.3
O#23	0.23	3.16	0.0	7.0	0.0	0.0	0.0	0.0	0.3	60.0	0.3	32.1	0.3
O#25	0.25	3.14	0.3	1.3	0.0	0.0	0.0	0.0	1.6	94.4	0.0	2.3	0.0
O#27	0.27	3.12	0.3	2.6	0.0	0.0	0.0	0.0	0.3	74.4	0.0	22.1	0.3
O#30	0.30	3.09	0.3	0.0	0.0	0.0	0.0	0.0	0.6	97.2	0.0	2.5	0.3
O#32	0.32	3.07	0.6	10.4	0.0	0.0	0.0	0.0	0.0	59.0	0.0	29.0	0.6
O#33	0.33	3.06	0.0	8.8	0.0	0.0	0.0	0.0	0.0	46.8	0.0	44.4	0.0
O#34	0.34	3.05	2.4	27.6	0.0	0.0	0.0	0.0	0.0	31.4	0.0	38.1	0.6
O#35	0.35	3.04	0.0	0.0	0.0	0.0	0.0	0.0	0.0	94.3	0.6	4.1	0.0
O#37	0.37	3.02	0.0	3.9	0.0	0.0	0.0	0.0	0.0	57.6	0.0	38.5	0.0
O#39	0.39	3.00	0.0	8.9	0.0	0.0	0.0	0.0	0.7	70.3	0.0	20.1	0.0
O#40	0.40	2.99	3.3	0.0	0.0	0.0	0.0	0.0	4.8	88.0	0.0	3.0	0.6
O#41	0.41	2.98	2.5	0.0	0.3	0.0	0.0	0.6	9.1	79.5	0.0	6.9	0.9
O#42	0.42	2.97	7.7	3.2	0.3	0.0	0.3	0.0	5.1	80.2	0.0	1.6	1.0
O#43	0.43	2.96	23.9	1.3	6.7	0.0	2.5	0.6	45.2	13.4	0.0	5.4	0.0
O#44	0.44	2.95	14.0	0.9	0.3	1.9	0.6	0.3	16.2	61.3	0.3	2.9	1.0
O#45	0.45	2.94	16.5	0.0	1.3	2.5	0.9	0.0	23.5	53.6	0.0	1.3	0.0
O#46	0.46	2.93	10.9	0.0	0.0	0.6	0.0	0.3	18.0	65.5	0.3	2.5	1.9
O#47	0.47	2.92	15.4	1.3	0.0	0.0	0.0	0.3	52.4	25.1	0.3	5.1	0.0
O#48	0.48	2.91	2.8	4.7	0.0	0.0	0.0	0.0	10.9	69.7	0.3	9.1	2.5
O#49	0.49	2.90	0.0	1.5	0.0	0.0	0.0	0.0	0.3	82.0	0.0	15.2	0.9
O#50	0.50	2.89	0.3	1.3	0.0	0.0	0.0	0.0	1.3	95.1	0.0	1.9	0.0

**Table 5**  
 $^{210}\text{Pb}_{\text{total}}$ ,  $^{40}\text{K}$ , and  $^{137}\text{Cs}$  content ( $\text{Bq kg}^{-1}$ ), Pb concentrations and Pb background values ( $\text{mg kg}^{-1}$ ) in the Ostrada core

Sample	Depth (m)	$^{210}\text{Pb}_{\text{total}}$	$^{40}\text{K}$	$^{137}\text{Cs}$	Pb	CRS age model	Error ( $\pm$ )	Inferred ages	Error ( $\pm$ )	Age model	Error ( $\pm$ )
O#1	0.01	71.02	998	11	69.14						
O#2	0.02	62.90	1053	11	70.85	2.33	1			2	1
O#3	0.03	66.18	1032	11	72.83	4.43	1			4	1
O#4	0.04	60.98	1009	12	76.55	6.62	1			7	1
O#5	0.05	57.93	976	12	81.19	9.12	1			9	1
O#6	0.06	52.94	997	13	89.84	11.78	1			12	1
O#7	0.07	57.33	1018	13	98.00	14.29	1			14	1
O#8	0.08	56.60	1075	20	107.31	17.37	1			17	1
O#9	0.09	59.40	1133	22	111.37	21.02	1			21	1
O#10	0.10	58.99	1099	26	119.39	24.70	1			25	1
O#11	0.11	60.65	1150	27	127.09	28.62	2	<b>25/34</b>	<b>3/7</b>	30	3
O#13	0.13	59.17	1188	18	108.06	33.68	2			34	2
O#15	0.15	52.96	1216	7	90.52	46.01	4	43	9	44	4
O#16	0.16	43.88	1307	5	80.93	66.98	7			60	7
O#17	0.17	42.60	1258	4	76.74	78.13	10			74	11
O#18	0.18	25.47	1320	5	70.51	98.60	17			89	17
O#19	0.19	21.36	1335	4	69.49	112.25	23			103	23
O#20	0.20				65.27					117	30
O#21	0.21	18.96	1338	3	66.44	147.53	39			131	37
O#23	0.23	–	–	–	59.97					160	50
O#25	0.25	13.54	1465	2	53.36	187.28	67	<b>176</b>	<b>20</b>	176	20
O#30	0.30	15.13	1422	0	42.62						
O#35	0.35	10.53	1397	0	31.30						
O#40	–	–	–	–	35.37						
		Median				Range					
Pb background		23				10–52					

Pb background values were calculated for the Basque estuaries by Cearreta et al. (2000). CRS age model with assigned errors and inferred ages from  $^{137}\text{Cs}$  (regular type) and Pb concentrations (bold type) are indicated. Age model is calculated from the sedimentation rates derived from the combination of  $^{210}\text{Pb}$ ,  $^{137}\text{Cs}$ , and Pb concentrations for the upper 15 cm, and  $^{210}\text{Pb}$  and Pb concentrations between 15 and 25 cm.

subsurface sharp peak at -10/-11 cm, before declining towards the surface. These results are in excellent agreement with CRS model derived age for the upper 15 cm. Table 5 summarizes the <sup>137</sup>Cs and <sup>210</sup>Pb data and Pb concentrations.

<sup>210</sup>Pb-derived dates and sedimentation rates are generally presented without error, producing a false sense of confidence in high-resolution studies (Gottgens et al., 1999). However, dating uncertainty increased with the age of the sediment, and even though estimates can be provided for up to 200 yr, they are associated to very large errors (c. ±70 yr), and therefore should be discarded. However, the initial increase in Pb concentrations over background values at -25 cm is in excellent agreement with the age provided by the CRS model, which allow us to consider 1820±20 AD as the best estimate, and therefore, we will use it in the sea-level reconstruction. Based on the sedimentation rates, the core could comprise more than 400 yr (Fig. 4). Based on the very good agreement between CRS, <sup>137</sup>Cs, and Pb concentrations derived sedimentation rates, we have used them for calculations of ages and errors (Table 5) that are shown in Figs. 4 and 5.

3.3. A foraminifera-based transfer function

There are differing opinions regarding the influence of elevation on foraminiferal distribution (Horton et al., 1999; Horton and Edwards, 2006). de Rijk (1995), and de Rijk and Troelstra (1997) suggested that key species correlated with environmental parameters such as salinity or sediment type rather than with elevation above mean tide level.

Most recent studies of modern distribution of salt marsh foraminifera are performed using samples taken along transects in marshes with a topographical gradient (e.g., Patterson et al., 2004; Vazquez et al., 2007). The main problem of this sampling strategy is the possible limitation for reconstructing past conditions when environmental controlling factors (i.e., elevation and salinity) are not orthogonal one to another in the training set (Loubere and Qian, 1997). Moreover, positive spatial autocorrelation (the tendency of sites close to each other to resemble one another more than randomly selected sites) is a property of most ecological data that makes the predictive power of some models over-optimistic and misleading. However, Telford and Birks (2005) stated the unimodal species–environment response models are more robust to autocorrelation.

Therefore, we selected different marsh areas with random sampling to avoid the intercorrelation of both elevation and salinity and possible autocorrelation. Additionally, combined training sets from various sites provide a more realistic analogue data for fossil assemblages, rather than local data sets (Gehrels et al., 2001).

Numerous methods have been developed to quantitatively reconstruct paleoenvironmental variables. Some of these have a stronger ecological and/or statistical basis than others. The fundamental distinction between existing methods concerns the underlying taxon–environment response model (Birks, 1995). We used detrended canonical correspondence analysis (DCCA) to determine if a unimodal (Gaussian) model or a linear response model of species to their environment is more appropriate. DCCA provides an estimate of the gradient length in relation to x in standard deviation (SD) units (Birks,

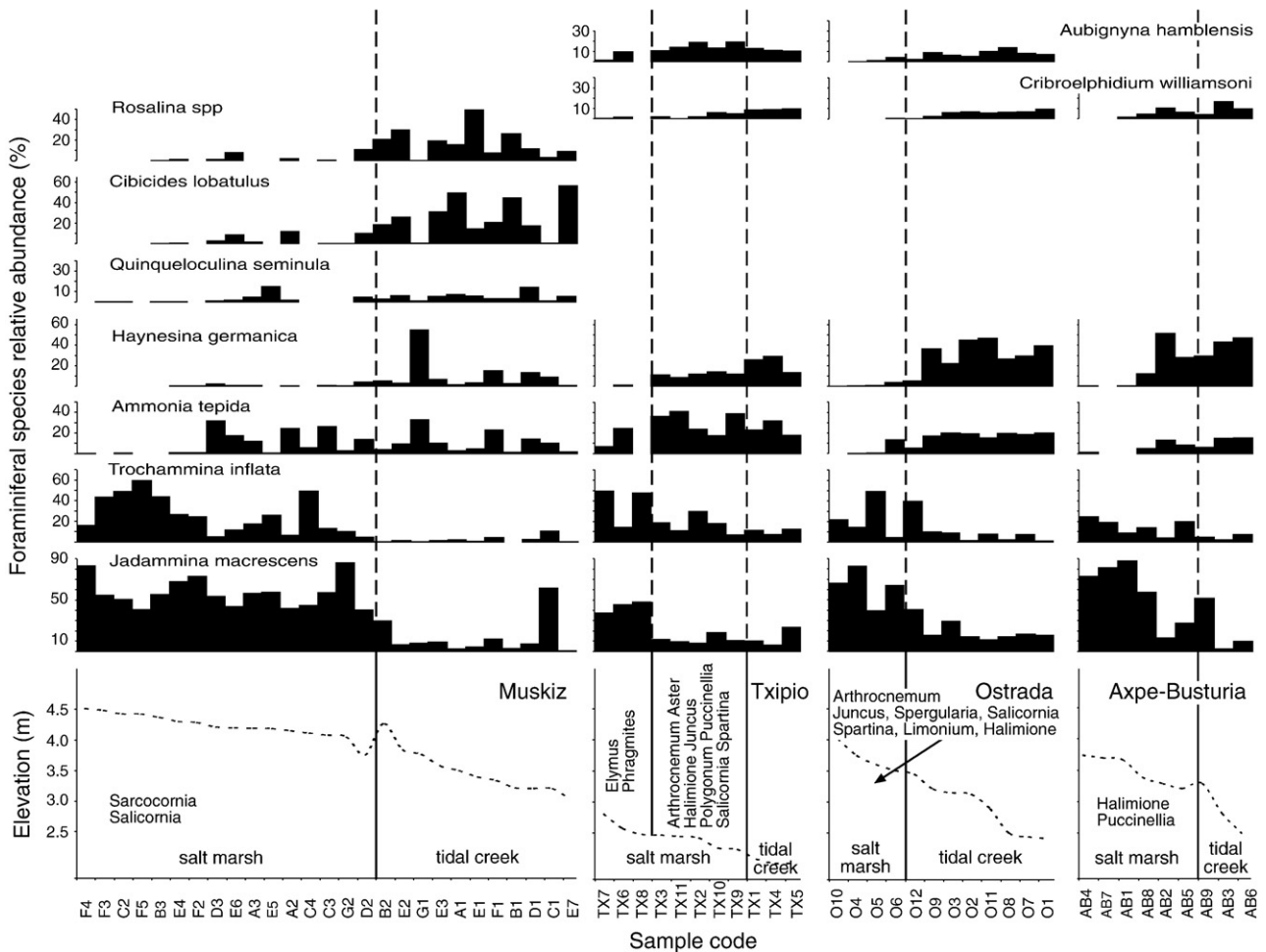


Fig. 2. Composition of dead foraminiferal assemblages from surface sediment samples related to local ordnance datum in the Muskiz marsh (Barbadun estuary), Txipio and Ostrada marshes (Plentzia estuary) and Axpe-Busturia marsh (Urdaibai estuary) showing relative abundance of the dominant species.

1995; Korsman and Birks, 1996). If the gradient length is longer than 2 SD units unimodal-based methods of regression and calibration are appropriate (Birks, 1995).

The performance of the transfer function was assessed in terms of the root-mean square of the error of prediction (RMSEP) and the squared correlation ( $r^2$ ) of observed versus predicted values. The RMSEP indicate the systematic differences in prediction errors, whereas the  $r^2$  measures the strength of the relationship of observed versus predicted values. These statistics were calculated as “apparent” measures in which the whole training set was used to generate the transfer function and assess the predictive ability, and the data were also jack-knifed (also known as ‘leave-one-out’ measures). Jack-knifing is a measure of the overall predictive abilities of the dataset. However, it does not provide sample-specific errors for the paleomorph elevation reconstructions of each core sample (Birks, 1995). Bootstrapping can be used to derive a standard error of prediction (SEpred; Birks et al., 1990; Line et al., 1994), which vary from sample to sample depending upon the composition of the core assemblage and the presence or absence of taxa with a particularly strong signal for the environmental variable of interest (Birks, 1995). SEpred was estimated using 1000 cycles.

We also employed the modern analogue technique (MAT; Juggins, 2004) to evaluate the likely reliability of paleomorph-surface elevation reconstructions based on the transfer function. The technique compares numerically, using chi-square distance dissimilarity coefficient, the foraminiferal assemblage in a fossil sample with the foraminiferal assemblages in all available modern samples. Through using the largest minimum dissimilarity coefficient (Woodroffe, 2006) we calculated if samples have good analogues in the training set (Horton and Edwards, 2006).

## 4. Results and discussion

### 4.1. Modern microfaunal content

Fig. 2 and Table 3 summarize the surficial results of dead foraminifera obtained from all four marshes. In the Muskiz marsh,

fifty eight different species of benthic foraminifera were found. Transported allochthonous species were moderate ( $9 \pm 15\%$ ; average  $\pm$  SD) from the vegetated marsh and decreased with increasing marsh elevation. Species diversity also decreased with increasing elevation in the marsh. The most abundant species found in the vegetated marsh were *Jadammina macrescens* ( $56 \pm 17\%$ ) and *Trochammina inflata* ( $20 \pm 19\%$ ). Agglutinated foraminifera dominated assemblages in the marsh ( $79 \pm 25\%$ ), although the calcareous component became more important in the lower samples of this subenvironment (e.g., *Ammonia tepida* was  $7 \pm 10\%$ ). In the tidal-creeks allochthonous species were very abundant ( $42 \pm 37\%$ ), and the main indigenous species were *J. macrescens* ( $21 \pm 24\%$ ), *A. tepida* ( $12 \pm 10\%$ ) and *Haynesina germanica* ( $9 \pm 5\%$ ). The porcellaneous component was represented mainly by *Quinqueloculina seminula* ( $4 \pm 4\%$ ).

In the Ostrada marsh, we identified thirty different species of benthic foraminifera. The abundance of allochthonous species was very low and decreased from an average of less than 2% in the tidal creeks to 0% in the vegetated marsh. Species diversity decreased with increasing elevation in the marsh. Assemblages were dominated by agglutinated foraminifera ( $92 \pm 15\%$ ), although a variable calcareous component was present in all samples. The most abundant species found in the vegetated marsh were *J. macrescens* ( $63 \pm 23\%$ ) and *T. inflata* ( $22 \pm 18\%$ ). Tidal-creek samples were dominated by hyaline foraminifera with *H. germanica* ( $31 \pm 14\%$ ), *A. tepida* ( $17 \pm 6\%$ ), *Aubignyna hamblensis* ( $6 \pm 3\%$ ) and *Criboelphidium oceanensis* ( $5 \pm 4\%$ ). The porcellaneous component was represented by *Q. seminula* ( $3 \pm 3\%$ ).

In the Txipio marsh, twenty eight different species of benthic foraminifera were identified. Allochthonous species were absent in the assemblages of the marginal marsh and very scarce in the other subenvironments ( $< 1\%$ ). Species diversity decreased with increasing elevation in the marsh. The most abundant species found in the marsh were agglutinated *J. macrescens* ( $44 \pm 9\%$ ) and *T. inflata* ( $37 \pm 18\%$ ) followed by hyaline *A. tepida* ( $10 \pm 12\%$ ). The low marsh was dominated by hyaline foraminifera with *A. tepida* ( $32 \pm 12\%$ ), *H. germanica* ( $12 \pm 3\%$ ) and *Criboelphidium williamsoni* ( $10 \pm 6\%$ ). Agglutinated foraminifera were represented by high amounts of *T. inflata* ( $17 \pm 9\%$ ) and *J. macrescens* ( $12 \pm 4\%$ ). The porcellaneous component was mainly

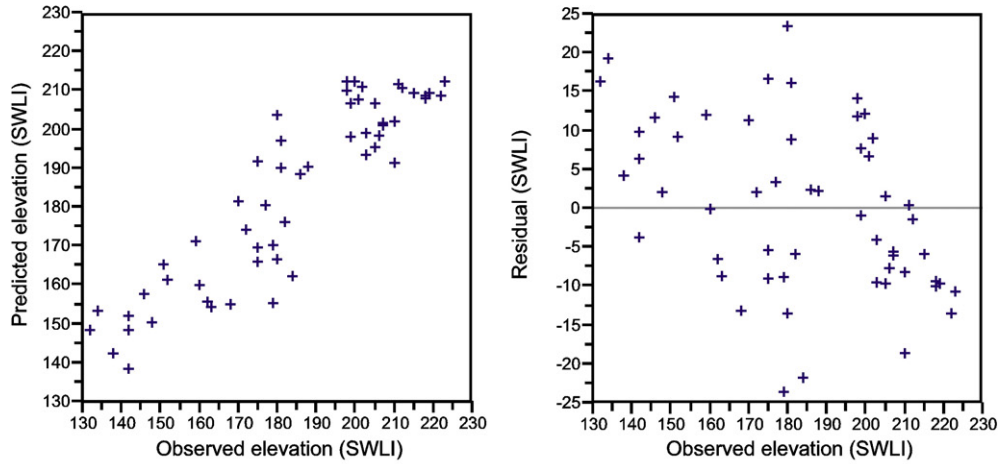
**Table 6**  
Statistics summary of the performance of WA, WA-Tol, and WA-PLS for the foraminiferal assemblages from the Basque marshes corresponding to Models 1, 2, and 3. WA: weighted averaging, WA-Tol: weighted averaging with tolerance downweighting, WA-PLS: weighted averaging-partial least squares

	RMSE	Max-Bias	$r^2$	Max-Bias <sub>jack</sub>	$r^2_{jack}$	RMSEP <sub>jack</sub>
WA	16.9892	15.283	0.69265	17.6812	0.647729	18.0054
WA-Tol	13.8093	24.7974	0.706831	26.7784	0.644165	15.2416
	Component 1	Component 2	Component 3	Component 4	Component 5	
<b>Model 1</b>						
RMSE	13.3494	12.1947	9.51148	9.09648	8.69816	
$R^2$	0.73575	0.77948	0.86584	0.8773	0.88781	
Max_Bias	23.791	16.7075	11.8347	11.9702	11.2038	
$r^2_{jack}$	0.68261	0.70749	<b>0.76931</b>	0.76869	0.73456	
Max_Bias <sub>jack</sub>	26.0011	18.8744	16.5372	19.4953	22.5905	
RMSEP <sub>jack</sub>	14.636	14.0655	<b>12.4991</b>	12.5664	13.5786	
<b>Model 2</b>						
RMSE	10.9689	10.6194	10.3899	10.3187	10.2844	
$R^2$	0.83393	0.84480	0.85191	0.85404	0.85489	
Max_Bias	16.4027	12.5931	11.5326	11.825	11.8287	
$r^2_{jack}$	<b>0.81201</b>	0.80561	0.80424	0.80818	0.80544	
Max_Bias <sub>jack</sub>	17.9664	14.0368	13.2005	13.5953	13.4922	
RMSEP <sub>jack</sub>	<b>11.6615</b>	11.8647	11.9078	11.8026	11.9137	
<b>Model 3</b>						
RMSE	7.6319	6.5124	5.7666	4.8076	4.6526	
$R^2$	0.7343	0.80657	0.8483	0.8945	0.9012	
Max_Bias	11.146	11.321	7.8331	6.4407	5.5599	
$r^2_{jack}$	0.6852	<b>0.7176</b>	<b>0.7496</b>	0.7037	0.6504	
Max_Bias <sub>jack</sub>	12.439	13.283	10.441	9.9049	16.192	
RMSEP <sub>jack</sub>	8.3254	<b>7.8757</b>	<b>7.4977</b>	8.4911	9.5444	

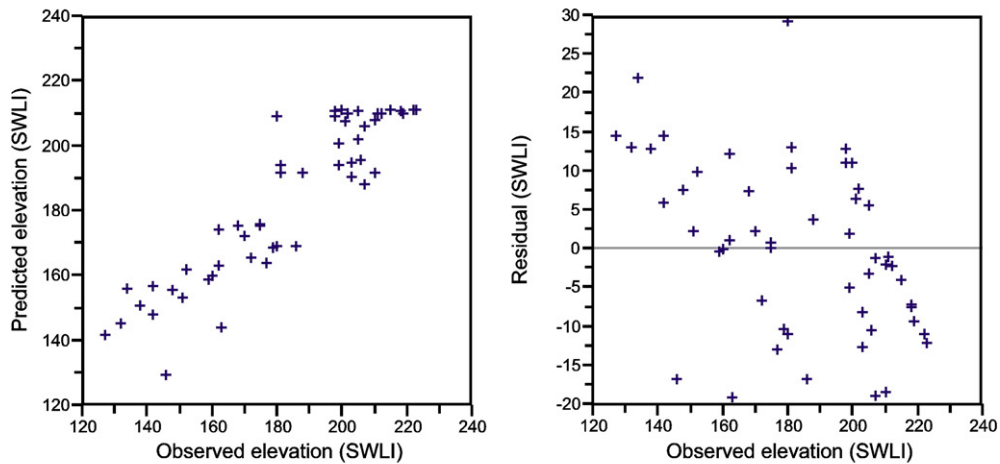
composed of *Q. seminula* (4±3%). The tidal-creek assemblages were also dominated by hyaline individuals but contained important amounts of agglutinated and low numbers of porcellaneous forami-

nifera. Dominant species were *A. tepida* (24±7%), *H. germanica* (23±10%), *J. macrescens* (13±10%), *T. inflata* (10±8%), *A. hamblensis* (9±7%) and *C. williamsoni* (9±3%).

### model 1



### model 2



### model 3

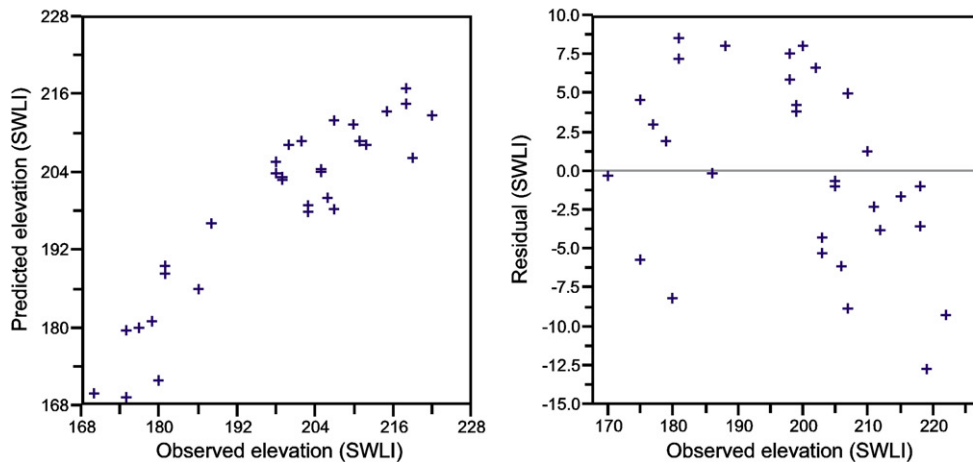


Fig. 3. Observed and predicted values of the SWLI for Models 1 (component 3), 2 (component 1) and 3 (component 3) of the foraminiferal transfer function (see Table 6 for  $r^2_{\text{jack}}$  values) and its residual errors.

In the Axpe–Busturia marsh, we identified twenty three different species of benthic foraminifera. Transported allochthonous species were absent in the high vegetated marsh and scarce in the other subenvironments (1% in the low marsh and 9% in the tidal creek). Species diversity decreased with increasing elevation in the marsh. The most abundant species found in the vegetated marsh were agglutinated *J. macrescens* (37±38%) and *T. inflata* (17±8%) followed by hyaline *A. tepida* (5±5%).

#### 4.2. Development of the foraminifera-based transfer function

DCCA of the training set with SWLI as the only environmental variable has produced a gradient length of 3.38. This indicates a unimodal nature of the foraminiferal abundance data with respect to SWLI. Thus, we used a unimodal-based method of regression and calibration, known as weighted averaging partial least squares (WA-PLS; Juggins, 2004), for the 59 samples and 23 species (>2%) obtained from Muskiz, Ostrada, Txipio and Axpe–Busturia marshes. This performed better than WA (Table 6). We did not screen any samples or species from the dataset (Model 1). The WA-PLS transfer function produces results for five components. The choice of component depends upon the prediction statistics (RMSEP and  $r^2$ ) and the principle of parsimony, i.e. choosing the lowest that gives an acceptable model. Using component three, the relationship between observed and foraminiferal-predicted elevation was very strong (Fig. 3), a result that illustrated the robust performance of the WA-PLS transfer function ( $r^2_{\text{jack}}=0.76$ ). These results indicated that reconstructions of former sea levels are possible (RMSEP<sub>jack</sub>=12.5).

We have further explored possible models that reconstruct paleomarsch-surface elevation. Model 2 uses only foraminiferal species typical from marsh environments, whereas Model 3 uses samples

above a standardized water level index of 160, thus removing lower elevation samples (see Hamilton and Shennan, 2005 for discussion) (Table 6). Model 2 performs significantly better (component 1;  $r^2_{\text{jack}}=0.81$ ; RMSEP<sub>jack</sub>=11.6) as result of including only species that respond to elevation, reducing therefore the noise of the dataset. Model 3 has low RMSEP (component 3; 7.5) but also low  $r^2_{\text{jack}}$  (component 3; 0.75) because of the lower number of samples and the reduced length of the elevational gradient.

The precision of the transfer functions is comparable to other foraminifera-based transfer functions from the northern Atlantic Ocean. Following back transformation of the SWLI values, Models 1, 2 and 3 have a precision of ±0.19 m, ±0.18 m and ±0.11 m, respectively. Horton et al. (1999) and Horton and Edwards (2006) recorded the foraminiferal assemblages from ten British and fifteen British and Irish coastal sites, respectively. The resulting transfer functions had a precision of ±0.12 m, although this value is dependant on local tidal range. Similarly, Gehrels et al. (2001) produced a foraminifera-based transfer function from three sites in the UK with a precision ranging from ±0.18 to ±0.29 m, while Massey et al. (2006) obtained a precision of ±0.29 m from two sites in the UK. On the other side of the Atlantic, Gehrels (2000) produced a foraminifera-based transfer function from 4 locations in Maine (USA) and Edwards et al. (2004) from 4 locations in Connecticut (USA) with a precision of ±0.25 m and ±0.18 m, respectively.

#### 4.3. Application of the foraminifera-based transfer function to reconstruct former sea levels

The Ostrada core was located at 3.391 m above local ordnance datum in the higher vegetated subenvironment of the seaward Ostrada unit (Fig. 1B). The sediment was composed of dark brown muddy silt

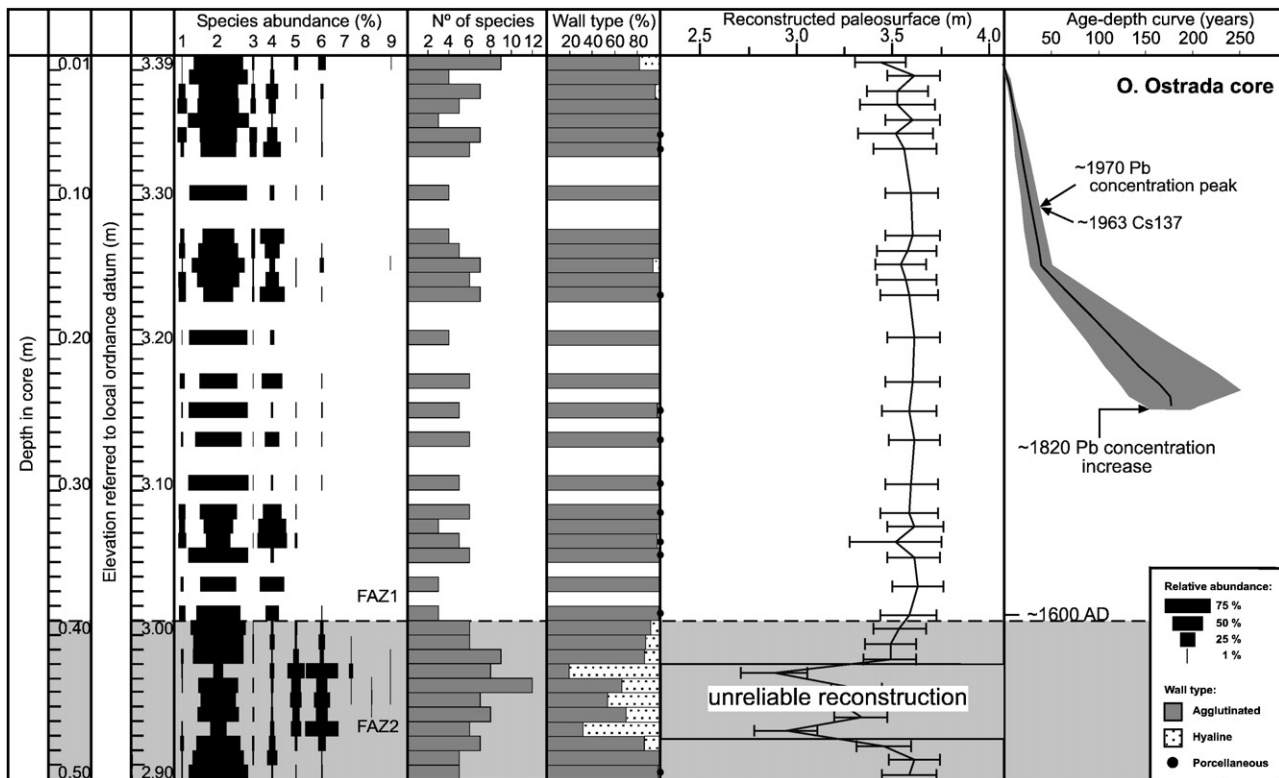
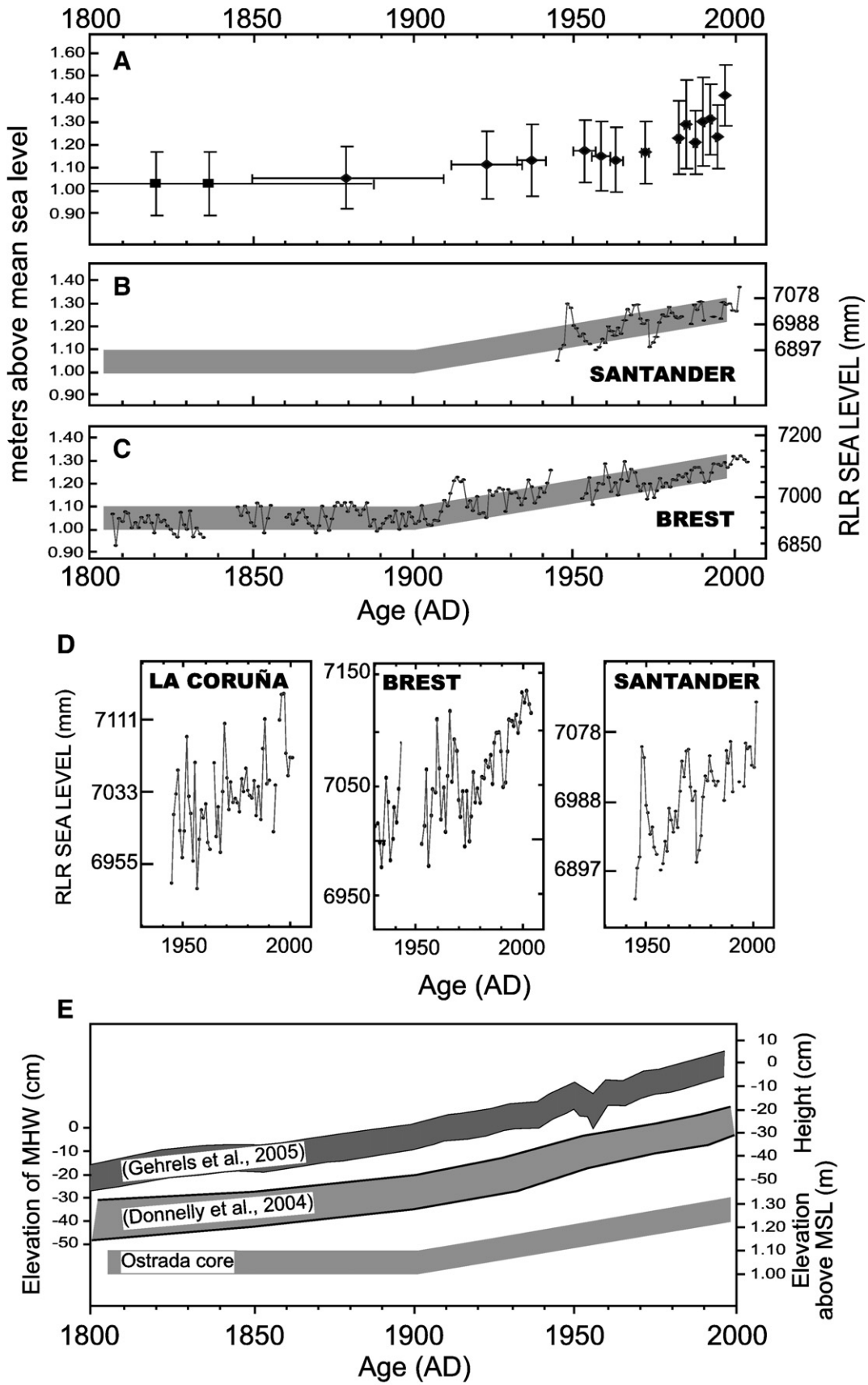


Fig. 4. Relative abundance of main foraminiferal species (1: *A. mexicana*; 2: *J. macrescens*; 3: *H. moniliforme*; 4: *T. inflata*; 5: *A. tepida*; 6: *H. germanica*; 7: *A. hamblensis*; 8: *C. oceanensis*; 9: *C. williamsoni*), number of species, wall type, predicted paleoelevation produced by the transfer function and sedimentation rates-derived age (Table 5) with depth (cm) referred to the local ordnance datum in the Ostrada core (Plentzia estuary). Predicted paleoelevation (continuous line) is presented with associated error margins. Black dots represent very low abundance of hyaline foraminifera in the sample. Age model chronology is represented as best fit line (continuous line) and errors (grey area). FAZ = Foraminiferal assemblage zone.



**Fig. 5.** Relative sea-level curve for the Ostrada core (Plentzia estuary) derived from the reconstruction of the elevations produced by the transfer function and from the age model chronology. Key: A—Ostrada sea-level reconstruction with assigned errors. B—Ostrada sea-level trend (derived from regression analysis, 95% confidence) for the 20th century and extrapolation to the 19th century versus annual values at the Santander tide gauge. C—Comparison between the Ostrada sea-level trend indicated in B and the annual values at the Brest tide gauge for the last ~200 yr. D—Comparison among the three longest tide-gauge records in the Bay of Biscay for the last ~50 yr: La Coruña, Brest and Santander. E—Sea-level general trends from northeastern North Atlantic, dark grey: Gehrels et al. (2005), light grey: Donnelly et al. (2004) compared to the Ostrada core sea-level trend.

with a small sand content (average  $4.5 \pm 4.3\%$ ) which increased between 39 and 50 cm (average  $8.4 \pm 1.1\%$ ) (Cearreta et al., 2002).

Twenty-three different species were found in the Ostrada core (Appendix A; Table 4) but only *J. macrescens* and *T. inflata* were dominant throughout (Fig. 4). The number of benthic foraminifera present in the Ostrada core was very high. Based on species distribution and lithological changes, Cearreta et al. (2002) differentiated two distinct foraminiferal assemblage zones (FAZ). FAZ2 is found between 50 and 39 cm and is characterized by a mixture of agglutinated ( $72 \pm 26\%$ ) and hyaline ( $28 \pm 26\%$ ) foraminifera. FAZ1 is found from 39 to 0 cm and is dominated by agglutinated foraminifera ( $98 \pm 4\%$ ) with *J. macrescens* ( $71 \pm 19\%$ ), *T. inflata* ( $20 \pm 14\%$ ) and *Arenoparrella mexicana* ( $6 \pm 7\%$ ) as the main species (Fig. 4). These species are indicative of a salt marsh environment. The agglutinated species *Hormosina moniliforme* is present throughout the core but becomes more abundant in the upper 17 cm ( $4 \pm 4\%$ ). A very small hyaline component is present in most samples ( $2 \pm 4\%$ ) with few tests of *H. germanica* and *A. tepida*. Foraminiferal density/50 g shows a general increasing tendency upwards with an average number of individuals of 850. Species diversity is very small (average number of species is 5), and the allochthonous foraminiferal content is null throughout the core.

We have selected Model 3 transfer function, which consists of modern samples from higher elevations (Table 6), to calibrate the foraminiferal assemblages because the sedimentological data suggest a salt marsh environment for the dated section of the Ostrada core. Furthermore, the fossil foraminiferal data have optima high in the tidal frame (above MHHW). The calibration process assigns a paleomarsch-surface elevation to each core sample together with bootstrapped standard error of prediction, which vary between 13 cm and 23 cm (Fig. 4). The foraminiferal assemblages are fairly similar throughout the FAZ1, except for the uppermost sample. Consequently, the transfer function predicts that the marsh surface at the sample site has varied little during the deposition of FAZ1, which indicates that the marsh surface has built up largely parallel to the sea-level rise. The highest ( $3.63 \pm 0.13$  m above local ordnance datum) and lowest ( $3.43 \pm 0.13$  m above local ordnance datum) reconstructed elevations (Fig. 4) are associated with relatively high abundances of *J. macrescens* and *T. inflata*, and *J. macrescens* and *H. germanica*, respectively. Other slight variations in the paleomarsch elevation reflect the presence of varying abundances in secondary species (e.g., the increase of *H. moniliformis* in the uppermost part of the core). FAZ2 is dominated by calcareous foraminifera, which modern analogues are not included in Model 3 transfer function. In contrast MAT indicates that all FAZ1 samples possess good modern analogues in the training set.

To illustrate fully the potential application of the transfer function technique, the foraminifera-based reconstructions from the Ostrada core were placed into a temporal framework to produce RSL reconstruction.

Fig. 5 represents the sea-level reconstruction since 1800 AD. Each foraminiferal sampling point is plotted as a sea-level index point using:

$$RSL_i = E_i - PME_i$$

where RSL is the former relative sea level for sample *i*, *E* is sample elevation in meters above the local datum for sample *i*, and PME is the paleomarsch elevation in meters above the local datum for sample *i* reconstructed by the transfer function.

We have used the Santander (the nearest to Ostrada marsh) and Brest tide gauges to assess the transfer function reconstruction of former sea-levels. Fig. 5 shows an excellent agreement between the instrumental and transfer function reconstructions, thus, high-resolution sea-level studies are possible in this region. Regression analysis through the mid-point of the reconstruction provides a

general trend of  $2.4 \pm 0.4$  mm yr<sup>-1</sup> for the period 1884–1997. From the dataset, the uppermost sample is a significant outlier, that if removed a new general trend of  $2.0 \pm 0.3$  mm yr<sup>-1</sup> is provided for the period 1884–1994. However, we have to consider the full vertical errors derived from the reconstruction, and therefore the error introduced into the calculated trend ( $\pm 78$  mm; Lyons, 1991). It should be noted that the three reconstructions of former sea level in the 19th century have very large temporal errors, and thus restrict considerably their interpretations during this century.

The Brest tide gauge data have been included in most GSLR studies (e.g., Barnett, 1984; Douglas, 2001; Nakada and Inoue, 2005; Church and White, 2006; IPCC, 2007) due to their completeness and accuracy since 1807 (Wöppelmann et al., 2006). Recently, Pouvreau et al. (2006) and Wöppelmann et al. (2006) presented new sea-level observations made in Brest since 1679, providing a data set that spans c. 300 yr. Wöppelmann et al. (2006) analyzed Brest data since 1807 and estimated a sea-level acceleration of  $0.007 \pm 0.008$  mm yr<sup>-2</sup> for the period 1807–2004. Additionally, they distinguished three linear trend periods: 1807–1890,  $-0.09 \pm 0.15$  mm yr<sup>-1</sup>; 1890–1980,  $+1.3 \pm 0.15$  mm yr<sup>-1</sup>; and 1980–2004,  $+3.0 \pm 0.5$  mm yr<sup>-1</sup>. The Santander tide gauge provides a trend of  $2.18 \pm 0.41$  mm yr<sup>-1</sup> for the period 1944–2001 (Table 1).

The likely increase in the rate of sea-level rise at the change of centuries is roughly coincident with the temperature increase during the 20th century (IPCC, 2007). This is also coincident with the onset of rapid recent sea-level rise reported in northeastern North America occurring between 1880 and 1920 (Donnelly et al., 2004; Gehrels et al., 2005) (see trends in Fig. 5). The similar timing for the onset of the recent sea-level rise at both sides of the (north) Atlantic Ocean proves the global significance and intensity of this acceleration of the sea-level rise. The different rates of sea-level rise detected geographically could be related to the different characteristics of the water masses and the influence of the North Atlantic Oscillation (Gehrels et al., 2006).

## 5. Conclusions

While accelerated rates of global relative sea-level rise are potentially one of the most devastating impacts of future climate change, our understanding of multi-decadal climate-ocean relationships is poor. This paper seeks to address this gap in knowledge by combining tide gauge and high-precision foraminifera-based transfer function reconstructions of RSL. In the Basque salt marshes foraminifera show a strong vertical zonation and the use of transfer functions has allowed the first quantitative estimate of sea-level index points for the Bay of Biscay. We have produced three transfer functions with a precision of between 0.19 m and 0.11 m. We placed the reconstructions of paleomarsch elevation into a temporal framework (<sup>137</sup>Cs, Pb concentrations, and <sup>210</sup>Pb-derived sediment accumulation rates) to produce former RSLs. The resulting RSL curve is in general agreement with the local tide gauge and the long-term regional gauge from Brest. Furthermore, it provides additional data to support that the actual rate of sea-level rise began between 1880 and 1920.

## Acknowledgements

Dr. Leorri was supported by a postdoctoral grant from the Basque Government (Spain) and by the Conseil Général of the Vendée (France). We thank Prof. Ronald E. Martin, Prof. Roland Gehrels, and Dr. Bruce Hayward for their comments and suggestions that greatly improved the original manuscript. We acknowledge and greatly appreciate research funding provided by a special topic award from the National Science Foundation (EAR-0713332). This work has been partially funded by the UNESCO06/08 and IT-332-07/GIU06-10 research contracts and it represents a contribution to IGCP project #495.

**Appendix A. Faunal reference list. M: Muskiz; T: Txipio; O: Ostrada; A: Axpe–Busturia; C: Ostrada core**

- Ammonia tepida* (Cushman) = *Nautilus beccarii* (Linné) var. *tepida* Cushman, 1926 (M, T, O, A, C)  
*Arenoparrella mexicana* (Kornfeld) = *Trochammina inflata* (Montagu) var. *mexicana* Kornfeld, 1931 (T, O, C)  
*Aubignyna hamblensis* Murray, Whittaker and Alve, 2000 (T, O, C)  
*Brizalina britannica* (Macfadyen) = *Textularia variabilis* Williamson var. *laevigata* Williamson, 1858 (M, T, O)  
*Cibicides lobatulus* (Walker and Jacob) = *Nautilus lobatulus* Walker and Jacob, 1798 (M, T, O, A, C)  
*Cibicoides pseudoungerianus* (Cushman) = *Cibicides pseudoungerianus* Cushman, 1922 (M)  
*Criboelphidium oceanensis* (d'Orbigny) = *Polystomella oceanensis* d'Orbigny, 1826 (M, T, O, A, C)  
*Criboelphidium williamsoni* Haynes, 1973 (M, T, O, A, C)  
*Fissurina lucida* (Williamson) = *Entosolenia marginata* (Montagu) var. *lucida* Williamson, 1848 (M, T, O, C)  
*Haynesina germanica* (Ehrenberg) = *Nonium germanicum* Ehrenberg, 1840 (M, T, O, A, C)  
*Hormosina moniliforme* (Siddall) = *Reophax moniliforme* Siddall, 1886 (T, O, C)  
*Jadammina macrescens* (Brady) = *Trochammina inflata* (Montagu) var. *macrescens* Brady, 1870 (M, T, O, A, C)  
*Massilina secans* (d'Orbigny) = *Quinqueloculina secans* d'Orbigny, 1826 (M, T, A)  
*Miliammina fusca* (Brady) = *Quinqueloculina fusca* Brady, 1870 (M, T, O, A, C)  
*Miliolinella subrotunda* (Montagu) = *Vermiculum subrotundum* Montagu, 1803 (M, T, A)  
*Planorbulina mediterraneanensis* d'Orbigny, 1826 (M, O)  
*Quinqueloculina lata* Terquem, 1876 (M)  
*Quinqueloculina oblonga* (Montagu) = *Vermiculum oblongum* Montagu, 1803 (M, T, C)  
*Quinqueloculina seminula* (Linné) = *Serpula seminulum* Linné, 1758 (M, T, O, A, C)  
*Quinqueloculina* sp2 (M)  
*Rosalina anomala* Terquem, 1875 (M, T, O, A)  
*Rosalina irregularis* (Rhumbler) = *Discorbina irregularis* Rhumbler, 1906 (M, T, O, A, C)  
*Textularia earlandi* Parker, 1952 (T, O, C)  
*Textularia saggitula* Defrance, 1824 (M)  
*Tiphrocha comprimata* (Cushman and Brönnimann) = *Trochammina comprimata* Cushman and Brönnimann, 1948 (O, C)  
*Trochammina inflata* (Montagu) = *Nautilus inflatus* Montagu, 1808 (M, T, O, A, C)

**References**

- Abril, J.M., 2004. Constraints on the use of <sup>137</sup>Cs as a time-marker to support CRS and SIT chronologies. *Environ. Pollut.* 129, 31–37.  
Allen, J.R.L., 1999. Geological impacts on coastal wetland landscapes: some general effects of sediment autocompaction in the Holocene of northwest Europe. *Holocene* 9, 1–12.  
Appleby, P.G., Oldfield, F., 1992. Applications of <sup>210</sup>Pb to sedimentation studies. In: Ivanovich, M., Harmon, R.S. (Eds.), *Uranium-series disequilibrium. Applications to Earth, Marine and Environmental Sciences*, 2nd edition. Oxford Science, Oxford, pp. 731–778.  
Barnett, T.P., 1984. The estimation of "global" sea level change: a problem of uniqueness. *J. Geophys. Res.* 89, 7980–7988.  
Benito, I., Onaindia, M., 1991. Estudio de la distribución de las plantas halófilas y su relación con los factores ambientales en la marisma de Mundaka-Urdaibai. Implicaciones en la gestión del medio natural. *Eusko Ikaskuntza, Cuadernos de Sección (Ciencias Naturales)*, p. 8 (116 pp.).  
Bindler, R., Renberg, I., Anderson, N.J., Appleby, P.G., Emteryd, O., Boyle, J., 2001. Pb isotope ratios of lake sediments in West Greenland: inferences on pollution sources. *Atmos. Environ.* 35, 4675–4685.  
Birks, H.J.B., 1995. Quantitative paleoenvironmental reconstructions. In: Maddy, D., Brew, J.S. (Eds.), *Statistical modelling of Quaternary science data. Technical Guide 5. Quaternary Research Association*, Cambridge, pp. 161–254.  
Birks, H.J.B., Line, J.M., Juggins, S., Stevenson, A.C., Ter Braak, C.J.F., 1990. Diatom and pH reconstruction. *Philos. Trans. R. Soc. Lond.* 327, 263–278.  
Boomer, I., Horton, B.P., 2006. Holocene relative sea-level movements along the North Norfolk Coast, UK. *Palaeogeogr. Palaeoclimatol. Palaeoecol.* 230, 32–51.  
Buzas, M.A., Hayek, L.C., Reed, S.A., Jett, J.A., 2002. Foraminiferal densities over five years in the Indian River, Lagoon, Florida: a model of pulsating patches. *J. Foraminiferal Res.* 32, 68–92.  
Cabanes, C., Cazenave, A., Le Provost, C., 2001. Sea level rise during past 40 years determined from satellite and in situ observations. *Science* 294, 840–842.  
Cazenave, A., Nerem, R.S., 2004. Present-day sea level change: observations and causes. *Rev. Geophys.* 42, 1–20.  
Cearreta, A., Irabien, M.J., Leorri, E., Yusta, I., Croudace, I.W., Cundy, A.B., 2000. Recent anthropogenic impacts on the Bilbao Estuary, Northern Spain: geochemical and microfossil evidence. *Est. Coast. Shelf Sci.* 50, 571–592.  
Cearreta, A., Irabien, M.J., Ulibarri, I., Yusta, I., Croudace, I.W., Cundy, A.B., 2002. Recent salt marsh development and natural regeneration of reclaimed areas in the Plentzia estuary, N. Spain. *Est. Coast. Shelf Sci.* 54, 863–886.  
Church, J.A., White, N.J., 2006. A 20th century acceleration in global sea-level rise. *Geophys. Res. Lett.* 33, L01602. doi:10.1029/2005GL024826.  
Church, J.A., White, N.J., Coleman, R., Lambeck, K., Mitrovica, J.X., 2004. Estimates of the regional distribution of sea level rise over the 1950–2000 period. *J. Clim.* 17, 2609–2625.  
Culver, S.J., Horton, B.P., 2005. Infaunal marsh foraminifera from the Outer Banks, North Carolina, USA. *J. Foraminiferal Res.* 35, 148–170.  
Cundy, A.B., Croudace, I.W., 1996. Sediment accretion and recent sea-level rise in the Solent, southern England: inferences from radiometric and geochemical studies. *Estuar. Coast. Shelf Sci.* 43, 449–467.  
Cundy, A.B., Collins, P.E.F., Turner, S.D., Croudace, I.W., Home, D., 1998. 100 years of environmental change in a coastal wetland, Augusta Bay, southeast Sicily: evidence from geochemical and paleoecological studies. In: Black, K.S., Paterson, D.M., Cramp, A. (Eds.), *Sedimentary processes in the intertidal zone. Geol. Soc. Lond. Spec. Publ.*, 139, pp. 243–254.  
de Rijk, S., 1995. Agglutinated foraminifera as indicators of salt marsh development in relation to late Holocene sea level rise (Great Marshes at Barnstable, Massachusetts). PhD dissertation, Vrije Universiteit Amsterdam, pp. 1–188.  
de Rijk, S., Troelstra, S.R., 1997. Salt marsh foraminifera from the Great Marshes, Massachusetts: environmental controls. *Palaeogeogr. Palaeoclimatol. Palaeoecol.* 130, 81–112.  
Donnelly, J.P., Cleary, P., Newby, P., Ettinger, R., 2004. Coupling instrumental and geological records of sea-level change: evidence from southern New England of an increase in the rate of sea-level rise in the late 19th century. *Geophys. Res. Lett.* 31, L05203. doi:10.1029/2003GL018933.  
Douglas, B.C., 1995. Global sea level change: determination and interpretation. *Rev. Geophys. suppl. U. S. National Report to International Union of Geodesy and Geophysics 1991–1994*, pp. 1425–1432.  
Douglas, B.C., 1997. Global sea rise: a redetermination. *Surv. Geophys.* 18 (2), 279–292.  
Douglas, B.C., 2001. Sea level change in the era of the recording tide gauge. In: Douglas, B.C., Kearney, M.S., Leatherman, S.P. (Eds.), *Sea Level Rise; History and Consequences*. Academic Press, San Diego, pp. 37–64.  
Duchemin, G., Joris, F.J., Redois, F., Debane, J.P., 2005. Foraminiferal microhabitats in a high marsh: consequences for reconstructing past sea levels. *Palaeogeogr. Palaeoclimatol. Palaeoecol.* 226, 167–185.  
Eades, L.J., Farmer, J.G., MacKenzie, A.B., Kirika, A., Bailey-Watts, A.E., 2002. Stable lead isotopic characterisation of the historical record of environmental lead contamination in dated freshwater lake sediment cores from northern and central Scotland. *Sci. Total Environ.* 292, 55–67.  
Edwards, R.J., van de Plassche, O., Gehrels, W.R., Wright, A.J., 2004. Assessing sea-level data from Connecticut, USA, using a foraminiferal transfer function for tide level. *Mar. Micropaleontol.* 51, 239–255.  
Farmer, J.G., Graham, M.C., Yafa, C., Cloy, J.M., Freeman, A.J., MacKenzie, A.B., 2006. Use of <sup>206</sup>Pb/<sup>207</sup>Pb ratios to investigate the surface integrity of peat cores used to study the recent depositional history and geochemical behaviour of inorganic elements in peat bogs. *Glob. Planet. Change* 53, 240–248.  
Flynn, W.W., 1968. Determination of low levels of <sup>210</sup>Po in environmental materials. *Anal. Chim. Acta.* 43, 221–227.  
Gehrels, W.R., 2000. Using foraminiferal transfer functions to produce high-resolution sea-level records from saltmarsh deposits, Maine, USA. *Holocene* 10, 367–376.  
Gehrels, W.R., 2004. Sea-level changes during the last millennium. In: Schwartz, M.L. (Ed.), *Encyclopaedia of Coastal Science*. Kluwer Academic, Dordrecht, pp. 1026–1030.  
Gehrels, W.R., Newman, S.W.G., 2004. Saltmarsh foraminifera in Ho Bugt, western Denmark, and their use as sea-level indicators. *Dan. J. Geogr.* 104, 49–58.  
Gehrels, W.R., Roe, H., Charman, D.J., 2001. Foraminifera, testate amoebae and diatoms as sea-level indicators in UK saltmarshes: a quantitative multiproxy approach. *J. Quat. Sci.* 16, 210–220.  
Gehrels, W.R., Belknap, D.F., Black, S., Newnham, R.M., 2002. Rapid sea-level rise in the Gulf of Maine, USA, since AD1800. *Holocene* 12, 383–389.  
Gehrels, W.R., Milne, G.A., Kirby, J.R., Patterson, R.T., Belknap, D.F., 2004. Late Holocene sea-level changes and isostatic crustal movements in Atlantic Canada. *Quat. Int.* 120, 79–89.  
Gehrels, W.R., Kirby, J.R., Prokoph, A., Newnham, R.M., Achterberg, E.P., Evans, H., Black, S., Scott, D.B., 2005. Onset of recent rapid sea-level rise in the western Atlantic Ocean. *Quat. Sci. Rev.* 24 (18–19), 2083–2100.  
Gehrels, W.R., Marshall, W.A., Gehrels, M.J., Larsen, G., Kirby, J.R., Eiriksson, J., Heinemeier, J., Shimmield, T., 2006. Rapid sea-level rise in the North Atlantic Ocean since the first half of the 19th century. *Holocene* 16, 948–964.  
Gobierno Vasco, 1986. Guía del medio ambiente natural de los municipios de Muskiz y Abanto y Zierbana. Servicio Central de Publicaciones del Gobierno Vasco, Vitoria, 119 pp.  
Gobierno Vasco, 1996. Catálogo abierto de espacios naturales relevantes de la Comunidad Autónoma del País Vasco. Servicio Central de Publicaciones del Gobierno Vasco, Vitoria, 635 pp.

- Gobierno Vasco, 1998. Avance del Plan Territorial Sectorial de Zonas Húmedas de la Comunidad Autónoma del País Vasco. Servicio de Publicaciones de la Administración de la Comunidad Autónoma del País Vasco, Vitoria-Gasteiz. (290 pp.).
- Gobierno Vasco, 1999. La red de vigilancia y control de la calidad de las aguas litorales del País Vasco. Años 1995–1996. Colección de recursos hídricos, 28. Servicio Central de Publicaciones del Gobierno Vasco, Vitoria, 96 pp.
- Goldberg, E.D., 1963. Geochronology with <sup>210</sup>Pb. In: IAEA (Ed.), Symposium on Radioactive dating, pp. 121–131 (Vienna).
- Goldstein, S.T., Watkins, G.T., Kuhn, R.M., 1995. Microhabitats of salt marsh foraminifera: St. Catherines Island, Georgia, USA. *Mar. Micropaleontol.* 26, 17–29.
- Gottgens, J.F., Rood, B.E., Delfino, J.J., 1999. Uncertainty in paleoecological studies of mercury in sediment cores. *Water Air Soil Pollut.* 110, 313–333.
- Hamilton, S., Shennan, I., 2005. Late Holocene relative sea-level changes and the earthquake deformation cycle around upper Cook inlet, Alaska. *Quat. Sci. Rev.* 24, 1479–1498.
- Hayward, B.W., Cochran, U., Southall, K., Wiggins, E., Grenfell, H.R., Sabaa, A., Shane, P.R., Gehrels, W.R., 2004. Micropaleontological evidence for Holocene earthquake history of the eastern Bay of Plenty, New Zealand, and a new index for determining the land elevation record. *Quat. Sci. Rev.* 23, 1651–1667.
- Hippensteel, S.P., Martin, R.E., Nikitina, D., Pizzuto, J., 2000. The transformation of Holocene marsh foraminifera assemblages, Middle Atlantic Coast, USA: implications for Holocene sea-level changes. *J. Foraminiferal Res.* 30, 272–293.
- Hippensteel, S.P., Martin, R.E., Nikitina, D., Pizzuto, J., 2002. Interannual variation of marsh foraminiferal assemblages (Bombay Hook National Wildlife Refuge, Smyrna, DE): do foraminiferal assemblages have a memory? *J. Foraminiferal Res.* 32, 97–109.
- Holgate, S.J., 2007. On the decadal rates of sea level change during the twentieth century. *Geophys. Res. Lett.* 34, L01602. doi:10.1029/2006GL028492.
- Horton, B.P., 1999. The contemporary distribution of intertidal foraminifera of Cowpen Marsh, Tees Estuary, UK: implications for studies of Holocene sea-level changes. *Palaeogeogr. Palaeoclimatol. Palaeoecol. Spec. Issue*, 149 (1–4), 127–149.
- Horton, B.P., Edwards, R.J., 2003. Seasonal distributions of foraminifera and their implications for sea-level studies. *SEPM Spec. Publ.* 75, 21–30.
- Horton, B.P., Edwards, R.J., 2006. Quantifying Holocene sea level change using intertidal foraminifera: lessons from the British Isles. *J. Foraminiferal Res. Spec. Publ.* 40 (97 pp.).
- Horton, B.P., Murray, J.W., 2006. Patterns in cumulative increase in live and dead species from foraminiferal time-series of Cowpen Marsh, Tees Estuary, UK: implications for sea-level studies. *Mar. Micropaleontol.* 58, 287–315.
- Horton, B.P., Edwards, R.J., Lloyd, J.M., 1999. A foraminiferal-based transfer function: implications for sea-level studies. *J. Foraminiferal Res.* 29, 117–129.
- Horton, B.P., Gibbard, P.L., Milne, G.M., Stargardt, J.M., 2005. Holocene sea levels and paleoenvironments of the Malay–Thai Peninsula, Southeast Asia. *Holocene* 15, 1199–1213.
- IPCC, 2007. Climate change 2007: the physical science basis. In: Solomon, S., Qin, D., Manning, M., Chen, Z., Marquis, M., Averyt, K.B., Tignor, M., Miller, H.L. (Eds.), Contribution of Working Group I to the Fourth Assessment Report of the Intergovernmental Panel on Climate Change. Cambridge University Press, Cambridge (996 pp.).
- Jennings, S.C., Carter, R.W.G., Orford, J.D., 1995. Implications for sea-level research of saltmarsh and mudflat accretionary processes along paraglacial barrier coasts. *Mar. Geol.* 124 (1–4), 129–136.
- Juggins, S., 2004. C2, Version 1.4: Newcastle University, UK, <http://www.campus.ncl.ac.uk/staff/Stephen.Juggins/index.html>.
- Kelly, D.L., Kolstad, C.D., Mitchell, G.T., 2005. Adjustment costs from environmental change. *J. Environ. Econ. Manage.* 50, 468–495.
- Korsman, T., Birks, H.J.B., 1996. Diatom-based water chemistry reconstructions from northern Sweden: a comparison of reconstruction techniques. *J. Paleolimnol.* 15, 65–77.
- Leorri, E., Cearreta, A., 2004. Foraminiferal interpretation of the Holocene environmental development of the Bilbao estuary, N. Spain. *Mar. Micropaleontol.* 51, 75–94.
- Leuliette, E., Nerem, R., Mitchum, G., 2004. Calibration of TOPEX/Poseidon and Jason Altimeter data to construct a continuous record of mean sea level change. *Mar. Geol.* 27 (1–2), 79–94.
- Line, J.M., Ter Braak, C.J.F., Birks, H.J.B., 1994. WACALIB version 3.3-A computer program to reconstruct environmental variables from fossil assemblages by weighted averaging and to derive sample-specific errors of prediction. *J. Paleolimnol.* 10, 147–152.
- Loubere, P., Qian, H., 1997. Reconstructing paleoecology and paleoenvironmental variable using factor analysis and regression: some limitations. *Mar. Micropaleontol.* 31, 205–217.
- Lyons, L., 1991. A Practical Guide to Data Analysis for Physical Science Students. Cambridge University Press, Cambridge. (107 pp.).
- Madariaga, I., 1995. Photosynthetic characteristics of phytoplankton during the development of a summer bloom in the Urdaibai Estuary, Bay of Biscay. *Estuar. Coast. Shelf Sci.* 40 (5), 559–575.
- Marcos, M., Gomis, D., Monserrat, S., Álvarez-Fajul, E., Pérez, B., García-Lafuente, J., 2005. Consistency of long sea-level time series in the northern coast of Spain. *J. Geophys. Res.* doi:10.1029/2004JC002522.
- Marcos, M., Wöppelmann, G., Bosch, W., Savcenko, R., 2007. Decadal sea level trends in the Bay of Biscay from tide gauges, GPS and TOPEX. *J. Mar. Syst.* doi:10.1016/j.jmarsys.2007.02.006.
- Marshall, W.A., Gehrels, W.R., Garnett, M.H., Freeman, S.P.H.T., Maden, C., Xu, S., 2007. The use of 'bomb spike' calibration and wiggle-matched high-precision AMS 14C analyses to date salt-marsh sediments deposited during the past three centuries. *Quat. Res.* 68, 325–337.
- Massey, A.C., Paul, M.A., Gehrels, W.R., Charman, D.J., 2006. Autocompaction in Holocene coastal back-barrier sediments from south Devon, south-west England, UK. *Mar. Geol.* 226, 225–241.
- Murray, J.W., 1991. Ecology and Paleoecology of Benthic Foraminifera. Longman, Harlow. (576 pp.).
- Murray, J.W., Bowser, S.S., 2000. Mortality, protoplasm decay rate, and reliability of staining techniques to recognize "living" foraminifera: a review. *J. Foraminiferal Res.* 30, 66–70.
- Nakada, M., Inoue, H., 2005. Rates and causes of recent global sea-level rise inferred from long tide gauge data records. *Quat. Sci. Rev.* 24, 1217–1222.
- Nerem, R.S., Leuliette, E., Cazenave, A., 2006. Present-day sea-level change: a review. *C. R. Geosci.* 338, 1077–1083.
- Onaindia, M., Amezcaga, I., 1999. Natural regeneration in saltmarshes of northern Spain. *Ann. Bot. Fennici* 36, 59–66.
- Patterson, R.T., Gehrels, W.R., Belknap, D.F., Dalby, A.P., 2004. The distribution of salt marsh foraminifera at Little Dipper Harbour, New Brunswick, Canada: implications for development of widely applicable transfer functions in sea-level research. *Quat. Int.* 120, 185–194.
- Paul, M.A., Barras, B.F., 1998. A geotechnical correction for postdepositional sediment compression: examples from the Forth valley, Scotland. *J. Quat. Sci.* 13, 171–176.
- Peltier, W.R., Tushingham, A.M., 1989. Global sea level rise and the greenhouse effect: might they be connected. *Science* 244, 806–810.
- Peltier, W.R., Jiang, X., 1997. Mantle viscosity, glacial isostatic adjustment and the eustatic level of the sea. *Surv. Geophys.* 18 (2), 239–277.
- Pizzuto, J.E., Schwendt, A.E., 1997. Mathematical modeling of autocompaction of a Holocene transgressive valley-fill deposit, Wolfe Glade. *Del. Geol.* 25, 57–60.
- Pouvreau, N., Minguéz, B.M., Simon, B., Wöppelmann, G., 2006. Évolution de l'onde semi-diurne M2 de la marée à Brest de 1846 à 2005. *C. R. Geosci.* 338, 802–808.
- Renberg, I., Brannvall, M.L., Bindler, R., Emteryd, O., 2002. Stable lead isotopes and lake sediments—a useful combination for the study of atmospheric lead pollution history. *Sci. Total Environ.* 292, 45–54.
- Ritchie, J.C., McHenry, J.R., 1990. Application of radioactive fallout Cesium-137 for measuring soil erosion and sediment accumulation rates and patterns: a review. *J. Environ. Qual.* 19, 215–233.
- Robbins, J.A., 1978. Geochemical and geophysical applications of radioactive lead. In: Nriagu, J.O. (Ed.), The biogeochemistry of lead in the environment, part A. Elsevier-North Holland Biomedical Press, Amsterdam, pp. 285–293.
- Scott, D.B., Leckie, R.M., 1990. Foraminiferal zonation of Great Sippewissett Salt Marsh (Falmouth, Massachusetts). *J. Foraminiferal Res.* 20, 248–266.
- Smith, J.N., 2001. Why should we believe 210Pb sediment geochronologies? *J. Environ. Radioact.* 55, 121–123.
- Tel, E., García, M.J., 2001. Mean sea level changes along the northern Iberian peninsular coast. Final Workshop of COST Action 40. Hydrographic Ins. of the Republic of Croatia.
- Telford, R.J., Birks, H.J.B., 2005. The secret assumption of transfer functions: problems with spatial autocorrelation in evaluating model performance. *Quat. Sci. Rev.* 24, 2173–2179.
- Tobin, R., Scott, D.B., Collins, E.S., Medioli, F.S., 2005. Infaunal benthic foraminifera in some north American marshes and their influence on fossil assemblages. *J. Foraminiferal Res.* 35, 130–147.
- Uriarte, I., Cotano, U., Villate, F., 2005. Effects of estuarine conditions and organic enrichment on the fecundity and hatching success of *Acartia clausi* in contrasting systems. *J. Exp. Mar. Biol. Ecol.* 320, 105–122.
- Valencia, V., Franco, J., 2004. Main characteristics of the water masses. In: Borja, A., Collins, M. (Eds.), Oceanography and Marine Environment of the Basque Country. Oceanography Series, vol. 70. Elsevier, Amsterdam, pp. 197–232.
- Valencia, V., Borja, A., Franco, J., Galparsoro, I., Tello, E., 2004. Medio físico y dinámica de los estuarios de la Costa Vasca. Aplicaciones en Ecología y Gestión. Report for the Departamento de Ordenación del Territorio y Medio Ambiente del Gobierno Vasco (92 pp.).
- Vazquez, N., Babalola, A.O., Boudreau, R.E.A., Patterson, R.T., Roe, H.M., Doherty, C., 2007. Modern distribution of salt marsh foraminifera and the cambesians in the Seymour–Belze Complex, British Columbia, Canada. *Mar. Geol.* 242, 39–63.
- Velicogna, I., Wahr, J., 2005. Greenland mass balance from GRACE. *Geophys. Res. Lett.* 32, L18505. doi:10.1029/2005GL023955.
- Velicogna, I., Wahr, J., 2006. Measurements of time-variable gravity show mass loss in Antarctica. *Science* 311, 1754–1756.
- Villate, F., Valencia, V., Urrutia, J., 1990. Estudio hidrográfico, sedimentológico y de metales pesados en las rías de Bidasoa y Plencia. Informes Técnicos del Departamento de Agricultura y Pesca del Gobierno Vasco, vol. 32 (100 pp.).
- Wahr, J., Swenson, S., Velicogna, I., 2006. The accuracy of GRACE mass estimates. *Geophys. Res. Lett.* 33, L06401. doi:10.1029/2004GL019779.
- Walton, W.R., 1952. Techniques for recognition of living foraminifera. *J. Foraminiferal Res. Spec. Publ.* 3, 56–60.
- Weiss, D., Shotky, W., Appleby, P.G., Kramers, J.D., Cheburkin, A.K., 1999. Atmospheric Pb since the Industrial Revolution recorded by five Swiss peat profiles: enrichment factors, fluxes, isotopic composition, and sources. *Environ. Sci. Technol.* 33, 1340–1352.
- Woodroffe, S.A., 2006. Holocene relative sea-level changes in Cleveland Bay, North Queensland, Australia: Unpublished Ph.D. Thesis. University of Durham, Durham, UK, 155 pp.
- Woodworth, P.L., 1990. A search for accelerations in records of European mean sea level. *Int. J. Climatol.* 10, 129–143.
- Wöppelmann, G., Pouvreau, N., Simon, B., 2006. Brest sea level record: a time series construction back to the early eighteenth century. *Ocean Dyn.* 56, 487–497.